Sensing and Bio-Sensing Research 29 (2020) 100348

Contents lists available at ScienceDirect

Sensing and Bio-Sensing Research

journal homepage: www.elsevier.com/locate/sbsr

Review article

Biosensing in dermal interstitial fluid using microneedle based electrochemical devices

Julia Madden[a,*], Conor O'Mahony[a], Michael Thompson[b], Alan O'Riordan[a], Paul Galvin[a]

[a] Tyndall National Institute, University College Cork, Ireland
[b] Department of Chemistry, University of Toronto, Canada

ARTICLE INFO

Keywords:
Dermal interstitial fluid
Electrochemical
Biosensor
Microneedle

ABSTRACT

This article explores recent advances in the development of electrochemical biosensors on microneedle platforms towards on-device sensing of biomarkers present in dermal interstitial fluid. The integration of a biosensor with a microneedle platform opens the possibility for minimally invasive bio-chemical detection or continuous monitoring within the dermal interstitial fluid. An introduction to interstitial fluid is provided placing emphasis on sampling methods that have been employed to extract and/or sample tissue fluid for analysis. We look briefly at microneedle technologies used to extract dermal interstitial fluid for subsequent analysis. Successive content will focus on microneedle technologies which have been integrated with electrochemical biosensors for the quantification of various metabolites, electrolytes and other miscellaneous entities known to be present in the dermal interstitial fluid. The review concludes with some of the key challenges and opportunities faced by this next-generation wearable sensing technology.

1. Introduction

Developments in wearable sensing technologies are becoming increasingly popular owing to their potential contribution to human health, performance and personalized medicine [1–3]. Those that are commercially available are mainly limited to measuring a real-time electrophysiological response. Electrophysiological parameters such as EEG (electroencephalography), ECG (electrocardiography) and EMG (electromyography), pulse oximetry and body temperature are some examples of physiological monitoring that can be measured with current wearable devices [4–6]. Previous reviews have described current developments in wearable sensor technologies covering aspects on fabrication [7], materials and systems [8], electrophysiological wearables [9], flexible wearables and electronics [10] sensors and electrochemical sensors [11], sweat monitoring [12], wireless and communications [13] as well as energy harvesting developments [14]. Conversely, this review explores advances specific to electrochemical sensors integrated with microneedles which are designed to interface with dermal interstitial fluid (ISF). Despite the tremendous growth in wearable sensor platforms, to date, there are a limited number of commercially available wearable devices capable of detecting or monitoring biomolecules [15]. Continuous glucose monitoring systems (CGM's) such as the Dexcom, Freestyle Libre and the Minimed are, to the best of the authors' knowledge, the only wearable devices on the market capable of monitoring at a molecular level [16]. These devices are described as minimally-invasive as the sensing element is inserted a couple of millimetres underneath the skin. Microneedles pose as an attractive wearable platform for molecular detection or monitoring as they have been integrated with biosensors capable of detecting metabolites, electrolytes and other clinically relevant targets. These devices differ from the current mini-needle devices as they are typically designed to extend no more than 1 mm into the skin potentially offering a less painful alternative [17,18]. This review is concerned specifically with microneedle technologies which have been fabricated to carry out bio-chemical measurements of various physiologically relevant targets present in the dermal ISF. Diagnostic testing for the presence of disease, whether of the genetic or infectious type is commonly performed through analysis of bio-fluids such as blood, urine and saliva [19]. Samples are collected from the patient and sent to a lab for analytical testing. ISF has received interest for the detection of analytes [20], biomarkers [21,22] metabolites [23] and drugs [24,25]. In particular, dermal or subcutaneous ISF is desirable as a medium for measuring physiological information in order to avoid repetitive blood extraction from patients [26]. Dermal or subcutaneous ISF can be accessed through the skin [25,27–29], however extraction techniques are not feasible for clinical use. Blood can be drawn directly from a patient in

* Corresponding author.
E-mail addresses: julia.madden@tyndall.ie (J. Madden), conor.omahony@tyndall.ie (C. O'Mahony), m.thompson@utoronto.ca (M. Thompson), alan.oriordan@tyndall.ie (A. O'Riordan), paul.galvin@tyndall.ie (P. Galvin).

https://doi.org/10.1016/j.sbsr.2020.100348
Received 17 January 2020; Received in revised form 10 May 2020; Accepted 13 May 2020

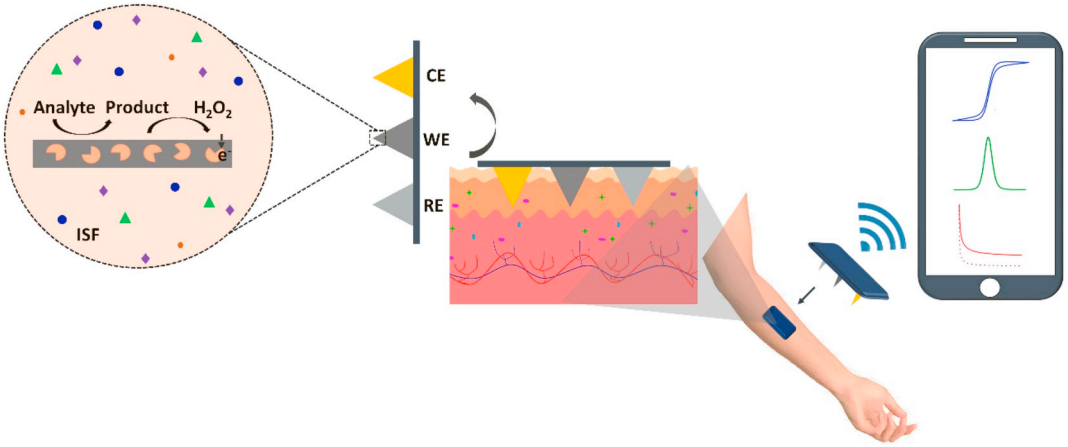

Fig. 1. Conceptualisation of a solid microneedle device worn on the human arm depicting the microneedles in the dermal interstitium and a simple representation of an oxidase-enzyme electrochemical reaction occurring at the microneedle/interstitial-fluid interface resulting in electrochemical data being collected and transmitted to a phone.

less than 3 min, by contrast, ISF extraction reports have listed various waiting times; from 10 min up to a number of hours. ISF extraction also yields low sample volumes depending on the device and method of extraction [30–32]. As a result, microneedles, which can directly interface electrochemical sensors with dermal ISF are being developed as wearable devices for bio-chemical based detection [33–35]. A conceptualisation of the use of solid microneedles for electrochemical detection within the dermal interstitium is depicted in Fig. 1. To gain a greater understanding of the potential for utilizing the interstitial space for wearable monitoring, this review will initially describe the ISF from a minimally invasive device perspective, and then focus on a number of research efforts which have accessed the fluid for molecular analysis. Later the review will highlight the role microneedles have played in accessing dermal tissue fluid as well as their integration with electrochemical sensors for detection and/or monitoring. Finally, the current status and the future perspective for these platforms will be summarised.

2. Interstitial fluid

Body fluid contents are broadly categorized either as extracellular fluid, i.e. the fluid surrounding all of the cells in the body, or intracellular fluid, i.e. the fluid contained within the cells in the body [36]. ISF, along with plasma, makes up the extracellular fluid environment. Fig. 2 depicts the distribution of water in the human body; the average human holds somewhere between 9 and 13.5 L of ISF [37,38].

Concepts on fluid filtration date back to the 1980s when Starling discovered that fluid injected into the interstitial space of a dog limb was present in venous blood [40]. Since then many advances in the understanding of fluid transport and the physiology of microvascular exchange have been well documented [41–44]. Fig. 3 illustrates fluid movement from the blood plasma through the endothelial cell wall in to the interstitial compartment/interstitium (region between the vasculature and cells) where it can access the lymphatic vasculature and return to the blood. Three paths exist for analytes to enter the interstitial fluid: firstly transcellular where diffusion occurs through the capillary endothelial cell wall; secondly, paracellular where they travel in between the cells, and lastly vesicular where analyte transport occurs from the cells to the ISF [45]. The interstitium is composed predominantly of a network of collagen, elastin, and glycosaminoglycans [46]. ISF resides within this network transporting metabolites and electrolytes to tissues, muscle cells, cartilage, bone cells, organs and other cell groups [38].

While there are a number of interstitial regions throughout the body

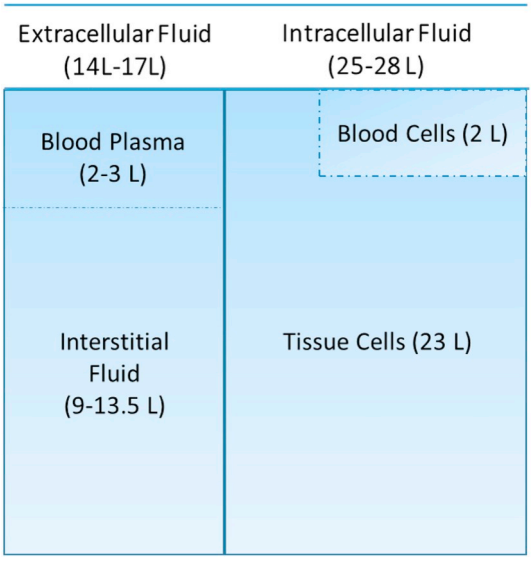

Fig. 2. Distribution of water in the human body showing the approximate volume of blood plasma and ISF in the extracellular fluid compartment, and the volume of tissue and blood cells in the intracellular fluid compartment, adapted from [39].

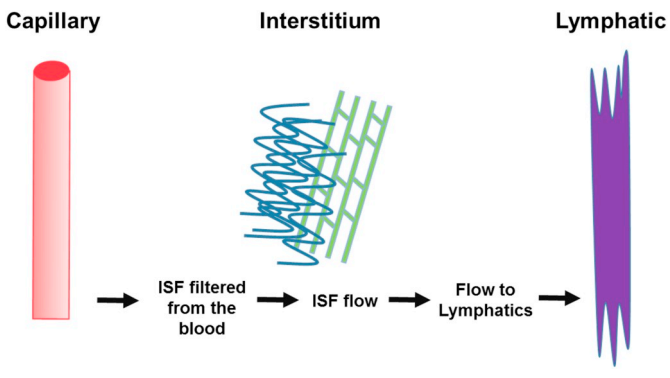

Fig. 3. Schematic representation of fluid flow to and from the interstitium, adapted from [46,47].

[42], interest for wearable devices is within the dermal and subcutaneous tissue compartments. Skin, the largest human organ, functions to protect internal tissues and organs. It is made up of three

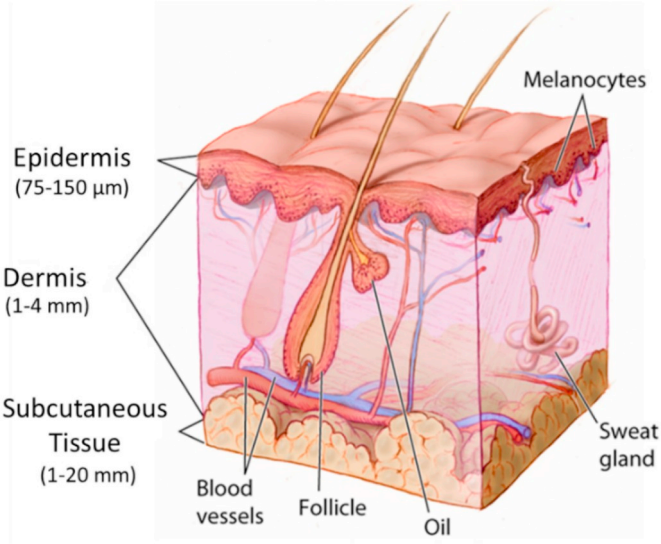

Fig. 4. Skin anatomy showing the outermost epidermal layer the epidermis, the dermis and the subcutaneous tissue which is also known as the hypodermis, adapted from [54].

primary layers as can be seen in Fig. 4. The outermost layer of the epidermis is the stratum corneum, which is made up of dead, keratin-filled cells, embedded in a lipid bilayer. The stratum corneum is approximately 10–20 µm in thickness [48], this layer prevents water loss from the body as well as acting as a barrier against external contaminants and environmental influences. Below the stratum corneum is the viable epidermis which is rich in immunologically-active cells such as Langerhans cells and is approximately 75–150 µm thick [49]. Finally, the dermis, which ranges from 1 to 4 mm in thickness [50] is the main structural connective tissue in the skin. The dermis is composed of fibroblasts, collagen fibres, elastic fibres, glyosaminoglycans, proteoglycans and is rich in blood and lymph vessels [49,51,52]. A real-time histological image of the dermal interstitial region can be seen in Fig. 5 [53]. Dermal ISF occupies the extracellular spaces between the cells, connective tissues and the vasculature. Both its location and its link with the vasculature system has resulted in research efforts towards developing extraction methods as well as attempts at understanding the relationship between plasma and ISF in terms of analytical composition.

2.1. Brief history of ISF sampling

Standardized techniques to access ISF through the skin have not been fully realised and represent something of a technical challenge. There are a limited number of methods which have been applied to the dermis for ISF extraction. One technique which continues to be applied for research purposes is the suction blister fluid method which involves the application of suction to the epidermal layer. This separates the epidermis and the dermis, creating a space in which ISF collects. Suction is then applied to the blister over time to collect the contained fluid [55,56]. Some disadvantages associated with this procedure are inflammation surrounding the blister, variations in blister size in addition to fluctuations in the volume of fluid collected [57]. Wick implantation is another method which requires the use of suction, in this instance blisters are not created; instead a nylon wick is firstly inserted into the dermal space so that ISF can be extracted directly to the wick [58]. Similarly, micropipettes have been used in conjunction with suction to obtain nL volumes from the skin [59]. These methods can result in discomfort to the patient as well as potentially providing inaccurate measurements from forced capillary filtration [60]. Hypodermic needles have also been applied 1.4 mm into the skin to extract dermal ISF in an attempt to compare glucose levels in ISF and venous blood. Extraction time was around 10 to 15 s. However, it yielded a volume of only 0.5 µL, which is considerably lower than the standard finger prick which yields up to 100 µL of capillary blood in seconds [61].The 'tissue cage reservoir' was another method examined for collecting dermal tissue fluid. The reservoir is made from a silicone based tubing, with pinholes in the size range of 0–2 mm on either side. This was implanted subcutaneously over a period of time until ISF built up in the tubing. Bio-fluid collection via device implantation is not a feasible practice for routine analysis of ISF [62]. The 'skin window technique', involved scraping away the epidermal layer of the forearm and placing a tissue culture chamber directly on to the dermal layer. Saline solution is added to the chamber, and, after some time, a quantity of this fluid is removed in order to introduce a negative pressure. This results in diffusion of the extracellular fluid into the chamber; this method is quite laborious, time consuming and un-suitable for clinical practice [63]. Venugopal et al. used near-IR laser to create micropores in the skin to which they subsequently applied a vacuum to extract the fluid. As this device penetrates the stratum corneum, it has been described as a painless technique. However an extraction time of 6 h yielded a sample volume of 60–90 µL [64]. Microdialysis and ultrafiltration are techniques which have been used to sample ISF for therapeutic diagnostic purposes. Both methods use a semipermeable membrane at the site of interest. In the case of microdialysis, the drug molecules diffuse across the membrane, whereas ultrafiltration applies a vacuum for extraction of the drug molecules [28,65,66]. Microdialysis has proven to be successful for drug monitoring at the site of interest and has been used in a number of pharmacokinetic studies [67,68]. From the techniques

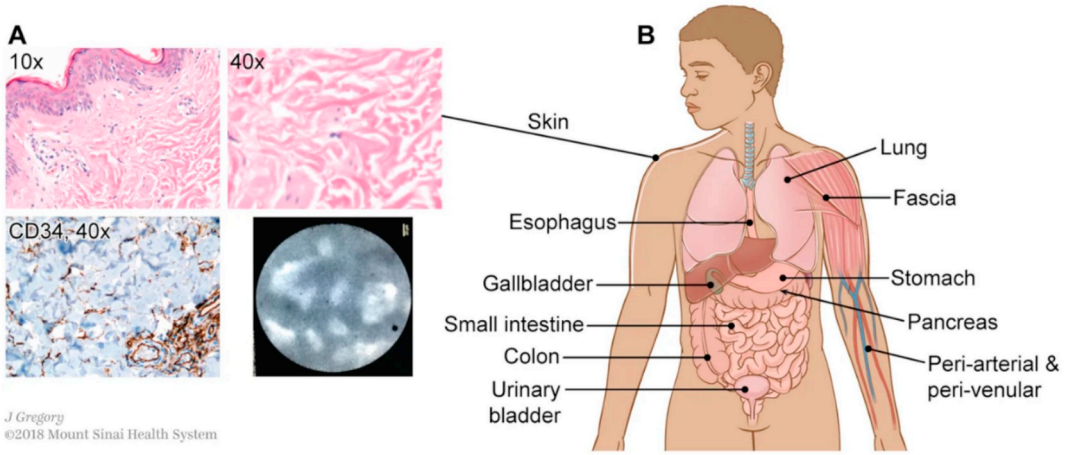

Fig. 5. Dermal interstitial space imaged using confocal laser endomicroscopy illustration by Jill Gregory, [53] (Open access).

Table 1
A summary of constituents which have been measured in ISF, their typical concentration levels, the sampling method applied and the quantification techniques [20,55,61,64,73].

ISF constituent	Measured concentration	Typical concentration ranges[a]	Sampling technique	Quantification technique	Subject tested
Glucose	4–8 mM	4.5–8 mM	Hypodermic needle	Manual hexokinase method	(Human n = 17)
Cholesterol	< 5.1 mM	1–5 mM	Microneedles	Commercial cholesterol kit	Mouse (n = 1)
Cortisol	24–40 nM	Morning: 1–50 nM Afternoon: 27–42 nM	Near-IR laser & vacuum pressure	ELISA & Electrochemical Impedance spectroscopy	Human (n = 6)
Lactate	1.17 ± 0.23 mM	1–2 mM	Microdialysis	Immobilized enzyme sensor technology (YSI 2700 Select)	Human (n = 15)
Lipids	1.5 ± 0.3 μM	Not reported	Suction blister	LC-Mass spectrometry	Human (n = 18)
Na^+	141 mM	135–150 mM	Suction blister	Glass Capillary Gas Chromatography-Mass Spectrometry	Human (n = 9)
K^+	4.4 mM	3.8–4.9 mM	Suction blister	Glass Capillary Gas Chromatography-Mass Spectrometry	Human (n = 9)
Cl^-	110 mM	99–117 mM	Suction blister	Glass Capillary Gas Chromatography-Mass Spectrometry	Human (n = 9)

[a] Typical concentration ranges for healthy individuals at rest.

described above, microdialysis has been the most successful in accessing ISF for analytes that accurately represent the levels present in the dermal tissue layer. Despite research efforts, there are no routinely practiced clinical extraction procedures which sample transdermal fluid for analysis, as a result, there is a limited amount of information on the analytical composition of tissue fluid. Table 1 provides some examples of target biomarkers which have been quantified in dermal ISF using various analytical methods. Microneedle platforms which have been developed to interface with ISF have become increasingly popular as a potential platform for sampling tissue fluid from the dermis [30] [69,70]. Further to this, through integration with electrochemical sensors, they open up the possibility for wearable bio-chemical detection within the dermal interstitium [71,72].

3. Microneedles

The stratum corneum prevents permeation of large, charged, and/or polar substances across the skin [74]. The microneedle transdermal delivery device was developed to combat this problem by creating transient micropores in the skin. These pores, the formation of which is painless to the user, increase the permeability of the skin by several orders of magnitude and close within hours [75–78]. Microneedles are described as microscopic, spike-like projections, generally less than 1 mm in height, and arrays of which are fabricated using a wide range of microfabrication techniques. The microneedle concept dates back to 1976 when a patent was filed on 'puncturing projections' by Gerstel and Place [79]. It was 1998 before the first proof of concept was demonstrated by Henry et al., whereby silicon microneedles were used to deliver the drug calcein [80]. Whilst microneedles refer to a specific type of device they have since been translated into a range of technologies for a variety of applications including cosmetic treatments [81,82], drug and vaccine delivery [83,84] ocular drug delivery [85], immunotherapy [86] electrophysiological sensing [87–89], ISF extraction [90] as well as bio-chemical sensing [91]. To the best of the authors' knowledge, no microneedle platform is commercially available for on-device ISF analysis. However there have been a few advances towards the approval of microneedles as transdermal delivery devices, for example, Nanopass technologies has received both CE marking and 510 k FDA approval for the Micron Jet which can deliver an influenza vaccine [92,93]. In addition to this, 3M, who have a cGMP manufacturing facility are currently involved in a phase III clinical trial with Radius health [94,95]. Solid microneedles produced by Seventh Sense Biosystems have also received FDA clearance and CE marking for a capillary blood sampling device using microneedles [71,96]. Table 2 depicts the current status of a number of microneedle technologies for various applications.

3.1. Fabrication and classification of Microneedle's towards ISF analysis

Detailed descriptions of several microneedle fabrication methods, materials used as well as information surrounding the classification of these devices are provided in number review articles [85,101–105]. Microneedles are most commonly fabricated from silicon, metals and polymers, however, ceramics, hydrogels, glass and composite based microneedles have also been reported [106,107]. Hollow, dissolvable, solid, coated and porous needles are examples of microneedle types cited in the literature [105]. Here, we will mention a number of fabrication technologies which have been used to produce microneedles specifically for ISF analysis. Both hollow and solid microneedles have been produced to interface biosensors with dermal tissue fluid. Silicon microneedles can be produced using a combination of common microfabrication processes (Fig. 6 A): photolithography, deep reactive ion etching, wet etching and plasma enhanced chemical vapour deposition (PECVD) [108,109]. This method of fabrication offers the possibility for wafer-scale production of microneedle devices [110] as well as the capabilities to fabricate both solid and/or hollow microneedles. Silicon is a well-established material used in both nano and micro fabrication processes where metal-oxide-semiconductor circuit technology can be used to enable device functionality [111]. Despite such advantages, the complex and timely nature of silicon processing as well as the cost of equipment has resulted in research efforts towards more cost effective microneedle fabrication methods such as drawing lithography and micromolding [112–118]. Chen et. al recently fabricated microneedles using a drawing lithography technique which incorporated magnetic particles in a polymer mixture. Through application of a magnetic field a 3D polymer structure is drawn away from the planar polymer surface (Fig. 6 B) [119]. This process can be carried out in one step and does not require expensive equipment [120], however further processing steps are required towards biosensor construction.

Other approaches such as cutting and machining of needles and attaching them via adhesion to a 3D printable [30] or a polymeric [121] base have also been described in the literature; whilst this is a straight forward and inexpensive approach, it is not easily scalable to high volume manufacturing. UV rapid prototyping is a technology which has successfully fabricated class II-A biocompatible hollow polymeric microneedles. This technique uses computer models to 3D print polymeric builds by guiding light over a photocurable material for selective polymerization [122]. Once the device has been electropolymerised it is subject to a cleaning step prior to curing. The steps involved in building 3D prototypes are few in comparison to the production of silicon (see Fig. 7 A) [123]. Solid polymeric microneedles are commonly fabricated from molding methods such as injection molding and micromolding. Generally speaking, the injection molding process

Table 2
Microneedle device technologies and their current status.

Device	Supplier	Description	Current status (development/certification/approval)	Application	References
Dermaroller®	Dermaroller GmbH	Solid polymeric and metal needles (200–250 μm)	Certified according to Annex V of the Medical Device Directive 93/42/EEG	Cosmetic – reduce wrinkle appearance	[97]
Microstructure Transdermal System®	3 M	Medical grade polymeric microneedles (1500 μm)	Initiated phase III of clinical trials in 2019 with Radius Pharmaceuticals	Transdermal delivery of Abaloparatide	[94,98]
Micron Jet®	Nanopass Technologies	Pure silicon crystal hollow microneedles (600 μm)	FDA clearance	Intradermal delivery of Influenza Vaccine	[93]
Microneedle Biosensor Array	Zimmer and Peacock	Solid microneedles functionalised to detect specific targets (e.g. glucose & lactate)	Not listed	Research and product developments for microneedle sensor based devices	[99]
TAP	Seventh Sense Biosystems	30 stainless steel solid microneedles (1000 μm)	FDA clearance	Blood capillary extraction	[71,96]
Intracutaneous Microneedle System	Zosano Pharma	Titanium microneedles (500 μm)	Completed phase III clinical trials in 2019	Transdermal delivery of Zolmitriptan	[94,100]

involves heating a material to its melting temperature T_m and subsequently adjusting the processing temperature in order to inject the material into a mold at a given speed. Although injection molding equipment are expensive they are compatible with large scale manufacturing [124,125]. Polycarbonate microneedles have been produced via injection molding at a production time of 12 s per sample proving to be appropriate for scalable manufacturing [125]. Micromolding methods employ solid microneedle structures to fabricate an inverse mold which is often formed from an elastomer [112]. This mold is then used to cast materials such as gold inks, polymers, composites or mixtures of materials [112–114,126] with biomolecules required for detection (see Fig. 7 B) [127] [114]. Once the material is applied to the mold, it can be subject to an external force such as centrifugal forces, compression or vacuum which are applied to ensure the mold cavities are filled. The material is then cured and allowed to cool prior to separation from the mold. In comparison to other fabrication methods this technique is relatively in-expensive, involves less complex processing steps and few equipment requirements.

Specific to ISF analysis, microneedles can be broadly summarised into two categories, firstly those used to extract or sample ISF for subsequent analysis and secondly those used to interface the ISF with on-device sensor technologies. As previously noted, this review is focused on electrochemical sensors fabricated on microneedle platforms. However it is important to note that other sensing modalities such as optical detection have also been integrated with these devices [129]. In many cases, microneedles fabricated specifically for ISF sampling have been used with the assistance of microfluidics or diffusion assisted methods in order to interface ISF with an analytical tool, where examples of these can be seen in Fig. 8 A–C [27,30,60,130]. Those fabricated for on-device sensing commonly require further processing post fabrication. Hollow microneedles have been integrated with common electrode materials i.e. gold, platinum and carbon by embedding wires of metal or carbon pastes into the needle bore prior to biosensor construction (see Fig. 8 D–F). Solid microneedles, on the other hand, have been metallised directly using techniques such as e-beam evaporation and sputtering followed by biosensor modification steps or in some instances the needle material itself has been molded with the necessary biological recognition element (see Fig. 8 G–I).

3.2. Microneedles for ISF extraction

In an earlier section of the review, a number of ISF sampling techniques were described, here, we will provide a few examples of where microneedles have a been applied to extract tissue fluid for analytical measurements. Hydrogel forming microneedles have been inserted into skin where they swell as a result of ‘fluid uptake’. The patches were worn for various time periods (30 min up to 3 h) after oral dosing of caffeine or glucose. Caffeine levels were measured using HPLC and a standard glucose assay kit was used to quantify glucose concentrations. Whilst this study proved that hydrogel microneedles could be used to sample ISF as well as detect the presence of both caffeine and glucose, analytical levels measured did not correlate with plasma levels and a number of lengthy laboratory procedures were required [132]. Samant et al. have also demonstrated successful ISF collection with microneedles, where over 1 μL of tissue fluid was collected within 20 min from both pig cadaver skin and living human subjects. Similar to sampling techniques discussed in Section 2.1, these long extraction times and low volumes are not compatible with current medical practices [138,139]. Miller et al. successfully extracted ISF (up to 20 μL) from human subjects for proteomic and transcriptomic analysis. ISF flow to the collection capillary took 30–120 s followed by a further 10 to 15-min for 20 μL of the fluid to collect. In comparison to extraction methods discussed earlier, this technique allowed for extraction in less than 20 min, in addition to this, a larger quantity of ISF was obtained. Proteome and transcriptome information was acquired showing similarities between ISF, Serum and Plasma suggesting that ISF could be

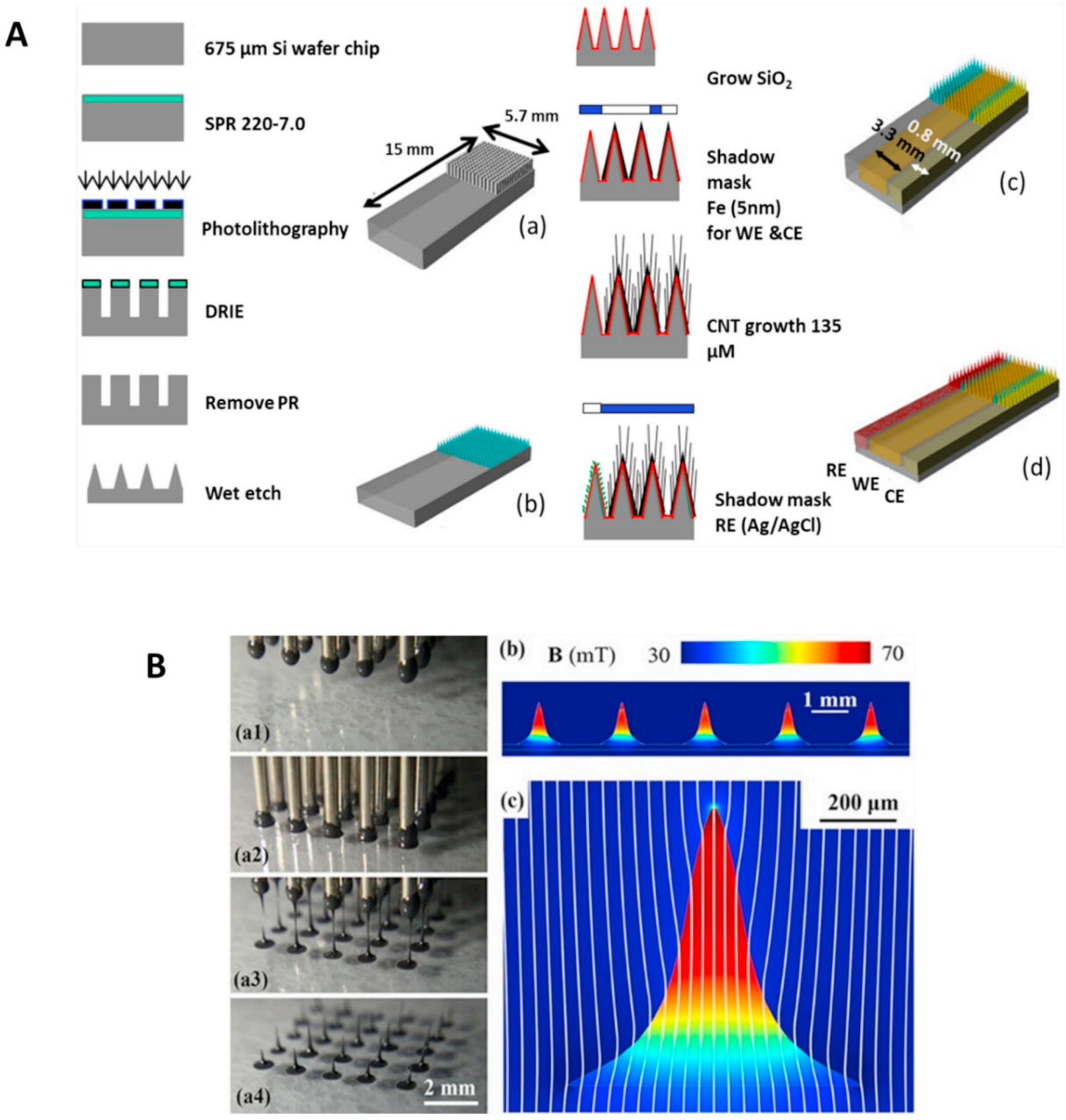

Fig. 6. A Fabrication sequence of the 3-electrode non-enzymatic microneedle-based glucose sensor (a) deep reactive ion etching of silicon to form rectangular pillar array; (b) wet etching of the rectangular pillar Si array to make sharp Si needle array; (c) iron deposition through a shadow mask and MWCNT growth followed by electroplating Pt nano-particles; and (d) Ag deposition through a shadow mask and formation of Ag/AgCl reference electrode, [108] (Open access), B (a1–4) Formation process of liquid MA using MDL method. (b, c) Magnetic field distribution in the liquid, [119] (Reprinted by kind permissions of and ACS publications).

used as an alternative bio-fluid for protein analysis [30]. Although these volumes are higher than those listed previously they are still relatively low in comparison to quantities of saliva, sputum, blood and urine routinely collected for examination. Applying sensors directly to the site of interest has the potential to eliminate the need for extraction and/or handling of tissue fluid. Currently, CGM devices are the only commercially available skin worn wearable device capable of on-device monitoring in tissue fluid. This technology contains a sensor which can penetrate up to 5 mm in to the skin [140]. In comparison, microneedles integrated with electrochemical sensors have been reported at heights ranging from a couple of hundred microns up to 1.5 mm [112,141], with some studies indicating that heights of less than 1000 µm are recommended for a more pain free user experience [142].

3.3. Hollow microneedles for electrochemical sensing applications

Whilst still at a relatively immature stage of development, microneedles fabricated and modified with electrochemical biosensor surfaces have demonstrated significant potential for on-device detection and/or monitoring of analytes present in tissue fluid. In order to functionalise hollow microneedles for electrochemical sensing, the lumen or bore of the microneedle can be modified to contain common electrode materials such as carbon, platinum and gold for subsequent functionalisation with biomolecules. A correlation found between blood and interstitial fluid alcohol levels has led to an interest in transdermal alcohol detection [143] using hollow microneedles fabricated from a liquid crystal polymer. 100-µm diameter wires were applied through

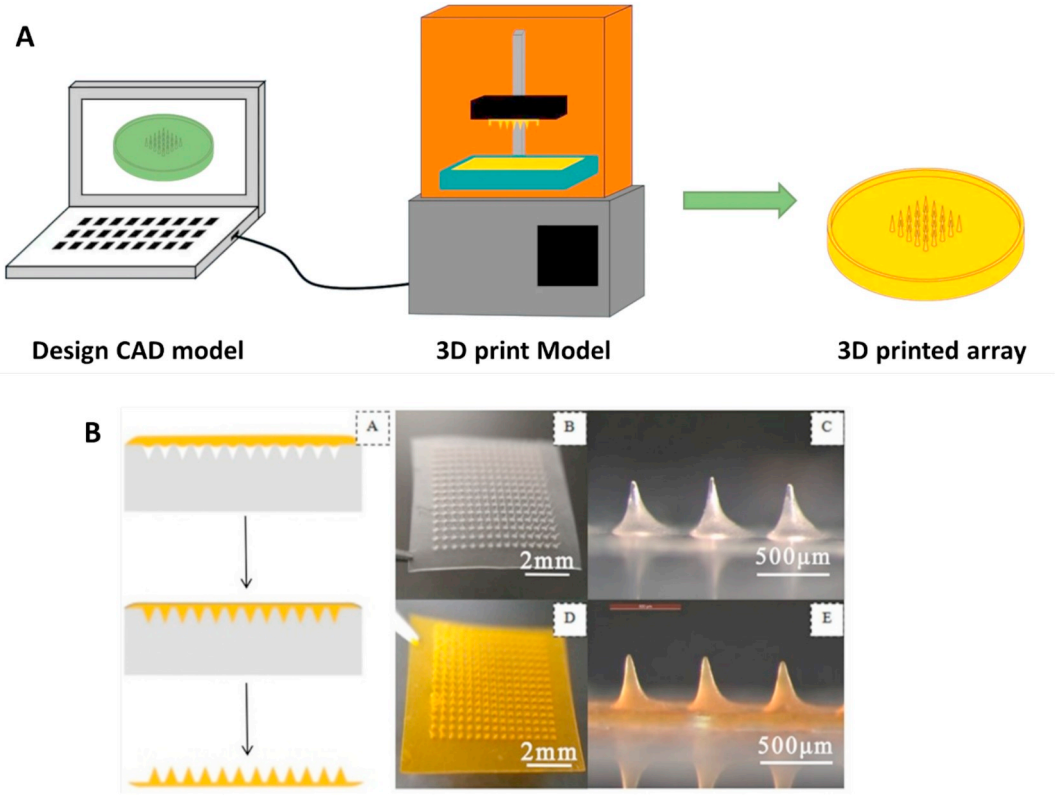

Fig. 7. A Needle array basin design followed by 3D printing of the design using a Form 2 SLA printer, adapted from [128], (Open access), B Schematic showing the preparation of silk fibroin microneedles: (A) schematic process of preparing needles, (B, C) images of 15 × 15 array produced via micromolding [127] (Reprinted by kind permissions of and ACS publications).

the needle bore, an illustration of these was seen in Fig. 8 E. Platinum wire, which is a biocompatible material, was used for both the counter and working electrodes and silver wire was employed as the reference electrode. Alcohol oxidase, the biomolecule required for detection, was deposited with chitosan on an o-phenylinediamine modified platinum working electrode. O-phenylinediamine can reduce interference from other common interfering species such as acetaminophen and L-ascorbic acid. Chitosan was used to immobilise/entrap the alcohol oxidase (AOx) on to the electrode surface. When producing sensors for direct contact with ISF, it is important that molecules do not leach from the device in to the microvasculature system. To prevent leaching of the alcohol oxidase enzyme a final modification of Nafion was deposited. Detection studies were carried out on artificial skin models and within artificial ISF (Table 3). Monitoring times of up to 100 min were achieved. A three electrode configuration on the microneedle platform, demonstrated on-device sensing capabilities, without the need for conventional reference and counter electrodes [134].

Hollow microneedles have also been fabricated to form part of a wearable device for melanoma detection [145]. A catechol-coated carbon-paste was embedded in the bore of one microneedle to function as the working electrode. Carbon paste was embedded in another needle to function as a counter and Ag/AgCl ink was inserted into the third microneedle as the reference electrode. The microneedles function to detect tyrosinase, an enzyme whose sensitivity is significantly increased in the case of primary melanoma. Catechol is oxidised to benzoquinone (BQ) following its interaction with tyrosinase resulting in the reduction of the BQ product. This reduction is measured amperometrically at the printed carbon working electrode as can be seen in Fig. 9 (D–F) [145]. Similar to the previous study, phantoms were used in an attempt to replicate the ISF and skin environment in order to assess the sensor response in a complex media. The majority of research articles discussed through-out this section focus on microneedle sensor developments with a bench top potentiostat which uses conventional electrochemical measurement methods. In order for a microneedle sensor to become a wearable, it must be integrated with the necessary electronic components. This study used a flexible electronic board to control the electrochemical measurements and data transmission. Whilst this device is solely suitable for single-use applications, it offers prospects towards cost effective wearable cancer screening technologies.

Hollow microneedles have also been combined with ion-selective-electrodes (ISE) for potassium detection. Electrolytes are attractive as a target for microneedle sensors as fluctuations in concentration levels can result from factors such as exercise, diet, disease and organ failure [146]. Here the ISE (composed of either porous carbon or porous graphene) was placed directly under a hollow microneedle. A microfluidic chip was used to extract fluid through a channel, towards the solid-state ISE where potassium levels were measured. Results showed that normal physiological potassium concentrations could be measured in the presence of interfering ions in standard solutions of known concentration. This technique required the use of vacuum and microfluidic valves as the sensor was embedded below the needle bores resulting in delayed measurements [146]. So far, we have seen that hollow microneedles combined with embedded electrochemical sensors can detect metabolites, cancer markers, and electrolytes, another significant example is drug detection. Levodopa (L-dopa) - a drug used in the management of Parkinson's disease has recently been measured with a wearable microneedle platform [141]. Optimizing L-dopa dosage is often dependent on a description of symptoms provided by patients which can be problematic towards appropriate treatment regimes. On this platform, two microneedles were modified to produce two working electrodes. One lumen was packed with a mixture of graphite paste, mineral oil and the enzyme tyrosinase to function as an enzymatic sensor for L-dopa detection (Fig. 10 B, E and H). The second working electrode contained a

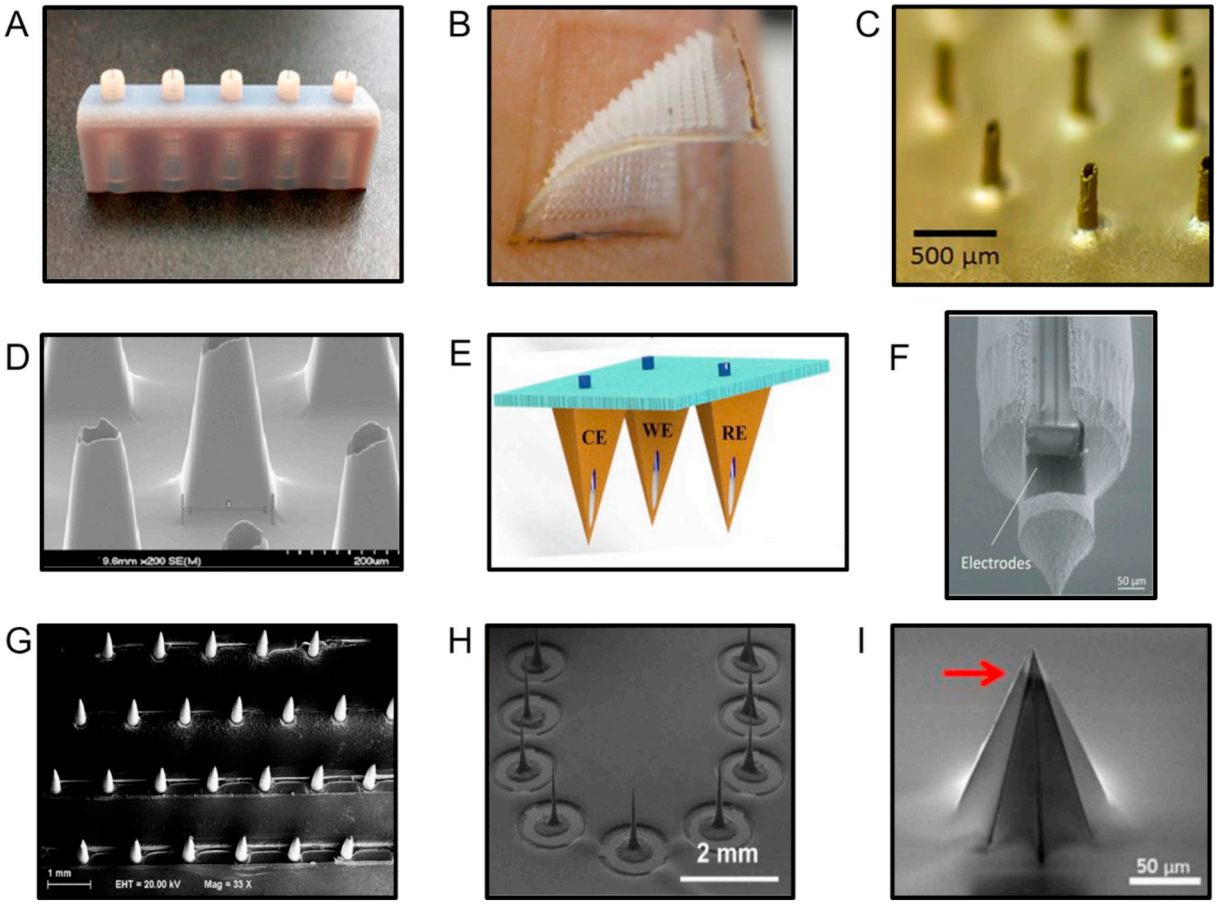

Fig. 8. Images A–C [129,131,132] depict microneedles which have been applied for ISF fluid extraction and subsequent analysis, (Reprinted by kind permissions of ACS publications, Plos one & Springer Nature) Images D–F [133–135] are hollow microneedles which have been integrated with electrochemical based sensors towards detection or monitoring within ISF, (Reprinted by kind permissions of Sage Journals, Elsevier & Springer Biomedical microdevices) and images G–I [113,136,137] show solid microneedles which have been modified through coating technologies and biosensor construction steps so that sensing or monitoring can be carried out at the interface between the solid microneedle and ISF, (Reprinted by kind permissions of ACS publications, Elsevier and the Electrochemical Society).

Table 3
Artificial ISF composition, Data from [144].

Constituent	mM	g/L
NaCl	107.7	6.3
KCl	3.48	0.26
$CaCl_2$	1.53	1.7 mLl (10% CaCl)
$MgSO_4$	0.69	0.17
$NaHSO_4$	26.2	2.2
NaH_2PO_4	1.67	0.26
$NaC_6H_{11}O_7$	9.64	2.1
Glucose	5.55	1
Sucrose	7.6	2.6

mixture of graphite paste and the mineral oil for non-enzymatic detection of L-dopa (Fig. 10, A, C and F). This dual sensor approach presents improved information gathering capabilities as well as a method of monitoring a second drug carbidopa. Measurements were carried out for up to 100 min demonstrating the potential for continuous drug monitoring. Appropriate concentration levels could be detected within artificial ISF through ex-vivo skin (Fig. 10 D) as well as phantom gels (Fig. 10 F), indicating suitability for further clinical evaluation [141]. Currently no data exists on L-dopa diffusion from blood to ISF; however it is thought that the short half-life of drug molecules could create problems for ISF drug monitoring as rapid fluctuations in drug concentrations can occur post administration [45].

Simultaneous screening on the one microneedle platform is also an attractive vision for future wearables. Hollow microneedles have been constructed for the simultaneous detection of vital diabetes markers: ketones, glucose and lactate. Ketone monitoring is required for the diagnosis of a life threatening condition, diabetic ketoacidosis. Conventionally, this is achieved through capillary measurement of β-hydroxybutyrate. At present there is no information on β-hydroxybutyrate levels in ISF; however, based on its small molecular size, it is thought to be close to that of plasma levels. CNC-machined hollow needles have been packed with carbon paste and later modified towards analysis of β-hydroxybutyrate, glucose and lactate. The modified biosensor layers for ketone and glucose detection are depicted in Fig. 11. This study detailed successful efforts to assess the sensor in a protein modified artificial ISF recipe over a prolonged period of 300 min [147].

There has been tremendous focus on developing various types of non-invasive wearable glucose monitoring systems on mouth guards, contact lenses and wearable sweat sensor patches to name a few [148–152]. A number of reviews have been published focusing primarily on microneedles for glucose detection [153–155]. Jina et al. demonstrated the use of hollow microneedles for true ISF glucose measurements. ISF diffused passively from the skin through the needle bore to a sensor housed underneath the needles. An image of this device was shown in Fig. 8 D [133]. A mean absolute relative difference of 15% was reported between ISF and capillary blood glucose levels. Similar to the platform discussed for melanoma detection, this device was assembled to contain the potentiostat circuit, a microprocessor to display and save the data and a battery. In this instance data were downloaded from the device as opposed to a wireless transmission. Up until now, each of the studies conducted measurements with

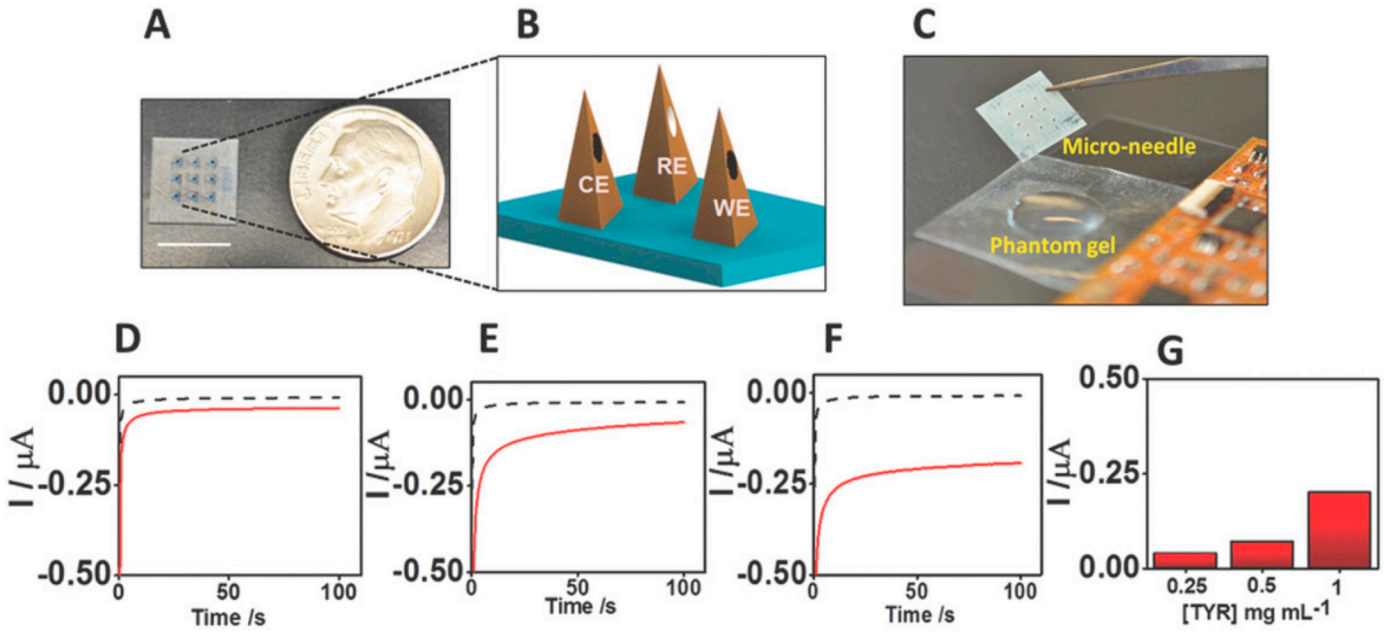

Fig. 9. Feasibility of transdermal tyrosinase screening in skin phantom gel using microneedle sensor. A Actual image of carbon paste packed hollow microneedle in comparison with a penny; scale bar = 1 cm. B Schematic of the pyramidal structure of the carbon filled microneedles surface with WE, CE, and RE. C Actual experimental setup mimicking skin phantom gel and microneedle used for tyrosinase detection with integrated electronic board. Amperometric response of different tyrosinase concentrations: D 0.25, E 0.5, and F 1 mg mL^{-1}, before (black line) and after (red line) interaction with skin phantom gel; G relative current values obtained from D to F amperogram, [145] (Reprinted by kind permissions of Wiley). (For interpretation of the references to colour in this figure legend, the reader is referred to the web version of this article.)

microneedles in buffer based solutions, artificial ISF, ex-vivo skin and in some instances phantom gels. This is one of few examples whereby a hollow microneedle patch is conducting electrochemical detection within a real ISF environment.

3.4. Solid microneedles for electrochemical sensing

Direct modification and functionalisation of solid microneedles with electrode materials is another approach for developing on-needle electrochemical sensors. This approach eliminates the need for packing micron sized bores with pastes and/or wires for front to back needle connection. Instead, techniques such as e-beam evaporation and sputtering can be used to form electrodes and interconnection tracks on the needles with the help of masking methods to ensure reproducible electrode fabrication. Sharma et al. have developed a glucose sensor on injection molded polycarbonate based microneedles. Four microneedle arrays were formed, three were metallised with Pt, one of which was used as a counter and the final array was metallised with silver to function as a reference electrode. The remaining platinum electrodes were modified via electropolymerisation of a glucose oxidase (GOx)/polyphenol mixture to produce two working electrodes. The device was capable of detecting glucose concentrations in buffer based solutions at physiologically relevant levels for ISF analysis (0-30 mM), with a response time of 15 s [156]. Entrapment is a common enzyme immobilisation strategy used in the development of microneedle devices, so as to physically restrict the enzyme from leaching. Further work evaluated its use as a wearable glucose sensor on human volunteers with Type 1 diabetes, in addition to healthy control patients. The intradermal measurements (Fig. 12) obtained from two working electrodes indicate comparable results between ISF and blood glucose measurements [35]. Testing was carried out for up to 20 h, with a lag of no more than 15 min. These results are promising towards the application of microneedles for continuous glucose monitoring; however, the durations of testing reported are not close to that of current CGM's which can function for 6–14 days [157].

Other investigations have taken a similar approach towards glucose detection on solid microneedles. Barrett et al. have fabricated solid electrochemical microneedles by implementing a low-cost micromolding polymer replication approach (as discussed in Section 3.1) for mediated glucose detection, using gold metallised microneedles as the working electrode, an external Ag/AgCl reference and a Pt wire as a counter electrode [137]. This work was furthered to conduct on-device glucose measurements by incorporating three electrode arrays on the one microneedle platform. However, this work is at preliminary stages with demonstrations of buffer based glucose detection at appropriate levels for ISF (0–19.5 mM) [126]. Attempts at non-enzymatic glucose sensors have also been demonstrated on solid stainless steel microneedles. These were modified with platinum and nafion for the direct electrochemical detection of glucose. Removal of the enzyme from the sensor surface allows for a more facile fabrication process avoiding the need to immobilise a biomolecule onto the needle surface post fabrication. This approach eliminates any risks associated with biomolecules leaching from the solid needles as well as reducing the biosensor construction costs. A linear response within the physiologically relevant ranges (1–40 mM) was achieved in buffer based solutions; however, this set-up employed an external Ag/AgCl RE and a Pt coil as the counter. Whilst successful glucose detection was achieved in blood samples, a 40% decrease in activity was reported after 12 continuous measurements proving to be disadvantageous towards continuous glucose monitoring applications [158]. Windmiller et al. developed the first solid polymer based microneedle tool capable of detecting both glutamate and glucose, with the potential for in-situ analysis. Glutamate, an excitatory neurotransmitter, is implicated in a number of medical conditions including heart attacks, strokes, and brain injury [159]. Both solid and hollow microneedles were fabricated using a rapid prototyping system. The hollow microneedles were used to mask all of the metallized regions on the solid microneedle substrate (Fig. 13 A and B), exposing only the microneedle metallic tips as sensor regions.

Here, the glutamate oxidase (GluOx) was immobilized via dip coating and GOx was immobilized using electrodeposition with both techniques entrapping the enzymes in *o*-phenyline diamine (Fig. 13 C). Measurements carried out in both phosphate buffers and undiluted

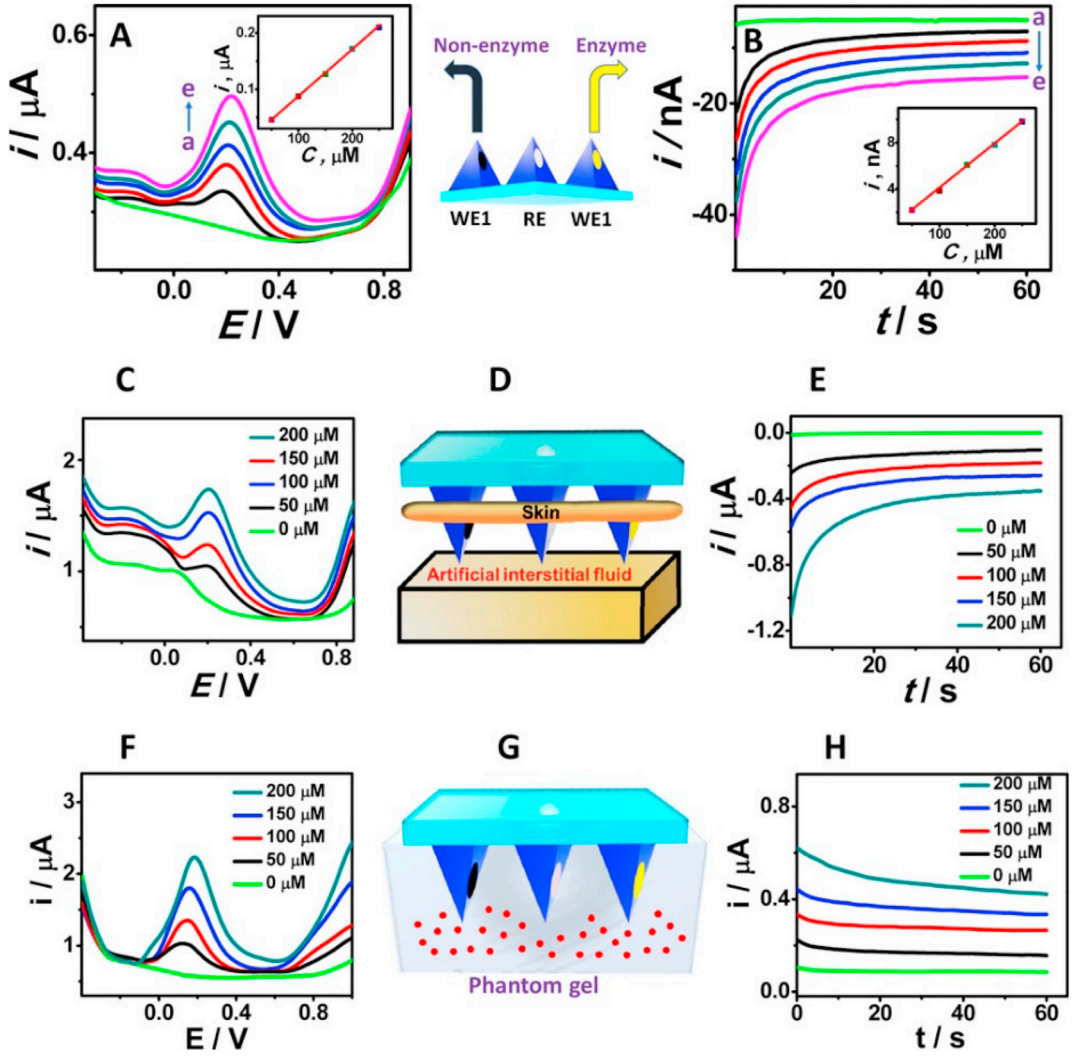

Fig. 10. A Square-wave voltammograms for Levodopa in ISF from 50 to 250 μM concentrations in 50 μM increments. (Inset shows the calibration plot of the background-subtracted peak-current vs L-Dopa concentration). B Chronoamperometry responses of the L-Dopa biosensor recorded in ISF from 50 to 250 μM in 20 μM increments at 0.3 V vs Ag/AgCl electrode. (Inset shows the corresponding calibration plots.) C, E Real-time L-Dopa detection in artificial ISF through the mice skin-penetrated microneedle. F, H SWV and amperometric responses of different L-Dopa concentrations with the mimicking-skin phantom gel. D Schematic showing the detection of L-Dopa in artificial ISF using the microneedle penetrated through the mice skin. G Schematic representation of the mimicking-skin phantom gel with the penetration of the microneedle, [141] (Reprinted by kind permission of ACS publications).

human serum samples indicated that the sensor was stable for up to 8 h and could function in complex bio-fluids; however no information was provided surrounding the plasma/ISF glutamate relationship [160]. Another metabolite receiving interest for microneedle sensors is lactate as it is often monitored for diseases such as cancer, obesity and diabetes [161]. It has also been a target of interest in the field of sports science [162,163]. Little data exists on the correlation between lactate levels in plasma and ISF, yet, its low molecular weight and high diffusivity indicate that concentration levels should be similar [45]. In work carried out by Caliò et al., polymer based microneedles were fabricated using photolithography methods whereby the enzymes lactate oxidase (LOx) and GOx were incorporated into a photocurable mixture [161]. Both lactate and glucose were amperometrically detected in buffer based solutions. The needles were molded from a material/biomolecule mixture reducing the need for additional functionalisation steps. This study showed a proof of concept with an external reference and counter as opposed to an on-device approach; however results were not entirely within the clinically relevant concentration ranges of 0.5–5 mM [164]. Another example of a lactate microneedle biosensor was developed by Bollella et al. [34,165] whereby polycarbonate microneedles were metallized with gold as the working electrode and an external reference was used for experimentation. The working electrode was functionalized via electrodeposition of gold multiwalled carbon nanotubes, followed by an electropolymerisation with methylene blue, and finally chemical attachment via drop casting of the enzyme. This device was found to function within a linear range of 0 to 100 μM in solutions of artificial ISF as well as human blood serum [165]. Again these levels are not within the appropriate ranges for lactate measurements. A decrease in signal was observed for measurements conducted in human serum which can be expected considering a higher level of fluid complexity. It is well known that biofouling is a common phenomenon for electrodes interfacing with bio-fluids, and despite lower levels of protein existing in ISF, tests in human serum provide insight into potential fouling effects. This needle technology has also been functionalised towards monitoring β-lactam (penicillin) levels. Preliminary data was obtained during 5 h intradermal measurements from human volunteers with results demonstrating a similar pattern to penicillin levels measured in blood as well as within microdialysate samples (see Fig. 14) [116].

Microneedles fabricated using the magnetorheological drawing technique discussed in Section 3.1 demonstrated simultaneous detection of uric acid, glucose and cholesterol in spiked serum samples. No indication regarding the Plasma/ISF analyte relationship was provided

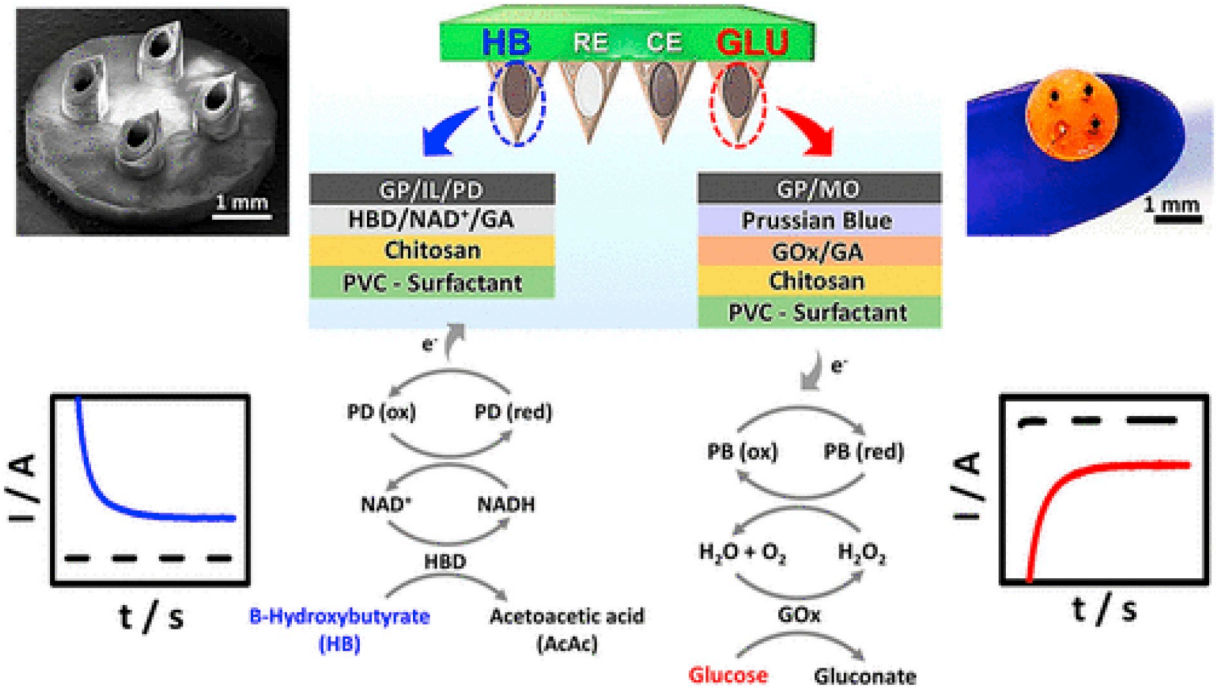

Fig. 11. Schematic representation of dual-marker HB/GL sensing on microneedle sensor platform. SEM image of the CNC-fabricated UCSD microneedle showing 2 × 2 array of hollow microneedles. The optical image of the microneedle sensor, showing the HB WE packed with GP/IL/PD, along with the GL WE filled with GP/MO paste and another GP/MO packed microneedle acting as the CE. An Ag/AgCl wire (500 μm)-integrated microneedle acts as the RE. The schematic illustration of the dual-analyte amperometric detection mechanism on multilayer modified sensors for HB (left) and GL (right). Also shown are typical amperograms obtained for HB (left) and GL (right) detection, [147].
Reprinted by kind permission of ACS publications.

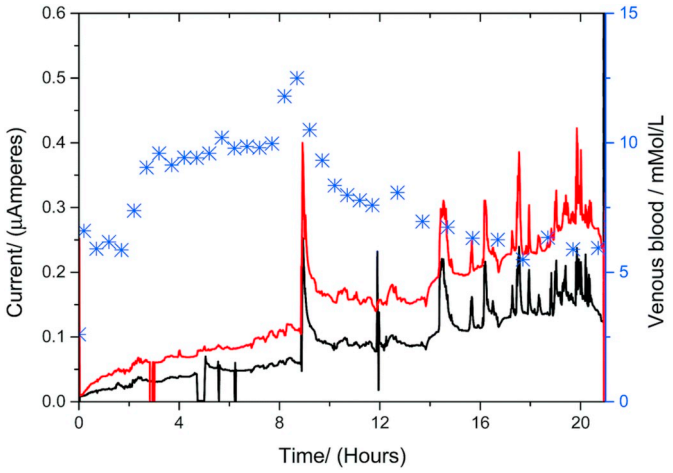

Fig. 12. Double axis plot representing chronoamperometric measurements from two sensors (black: working electrode 1; red: working electrode 2) on the same device versus glucose measurements from venous blood (blue stars), [35]. (For interpretation of the references to colour in this figure legend, the reader is referred to the web version of this article.)
Reprinted by kind permission of The Royal Society of Chemistry.

for any of the analytes; however, this work demonstrated portable simultaneous sensing capabilities on one microneedle platform with a portable electroanalyser [136]. As previously mentioned, few articles detail efforts to integrate microneedle electrochemical sensor platforms with the necessary electronics to perform measurements without a bench top potentiostat. One recent example of wireless glucose detection within human serum was demonstrated using solid microneedles. The sensor was assembled with a miniaturised potentiostat for electrochemical measurements, an analog to digital convertor module, Bluetooth and a near-field communication (NFC) module as well as a miniaturised flexible battery [117]. It demonstrated significant potential as an integrated wearable platform capable of measuring bio-chemical signals and transmitting data in a readable format. However, similar to the majority of studies discussed, it was not subject to testing in the human dermal interstitium. The following tables provide a summary of recently published electrochemical based microneedle sensors fabricated from micromolding (Table 4), injection molding (Table 5) and other miscellaneous methods (Table 6) detailing the microneedle type, materials and biosensor layers a long with the concentrations ranges measured and those that are physiologically relevant.

4. Challenges and future perspectives

Significant advances have been made towards accessing and analysing dermal tissue fluid, yet, limited information exists for physiologically relevant ranges of analyte and drug concentrations. This information is vital towards diagnosing health conditions and physiological states. Much of the work carried out to date has been on the major metabolite glucose [168,169]. Further investigations into the clinical chemistry of tissue fluid may present other biomarkers of interest in ISF, as well as providing further insight into the current understanding on how biomarker tissue fluid levels relate to those of blood. ISF sampling practices can be time consuming with some of the more recent microneedle extraction studies showing times of 10 to 15 min to attain sufficient levels of fluid for analysis [30]. Furthermore, sampling methods collect relatively low volumes of the extracellular fluid. Extraction tools such as microneedle arrays and sonophoretic devices often require the use of a vacuum or suction to enhance permeability through the tissue matrix. These methods can result in patient discomfort as well as forced capillary filtration leading to inaccurate measurements [60]. Utilizing passive diffusion methods is far more desirable for direct sensing applications. For example Miller et al. collected ISF at volumes of up to 20 μL, without the need for a vacuum or

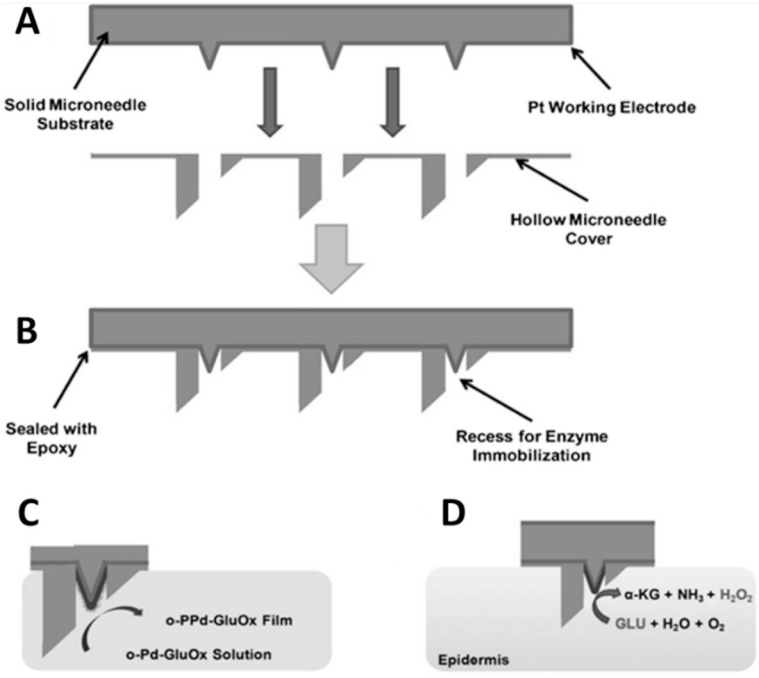

Fig. 13. (A) Solid and hollow microneedle constituents of the bi-component microneedle array electrode. (B) Fully-assembled bi-component microneedle array electrode. (C) Growth of the glutamate oxidase (GluOx)-functionalized poly(o-phenylenediamine) (PPD) film at the solid microneedle surface within the recess from the o-phenylenediamine (o-PD) monomer. (D) Biocatalytic behavior of the electropolymerized glutamate oxidase–poly(o-phenylenediamine) film (illustrated in purple), enabling the quantification of glutamate levels within the transdermal fluid, [160] (Reprinted by kind permission of Wiley). (For interpretation of the references to colour in this figure legend, the reader is referred to the web version of this article.)

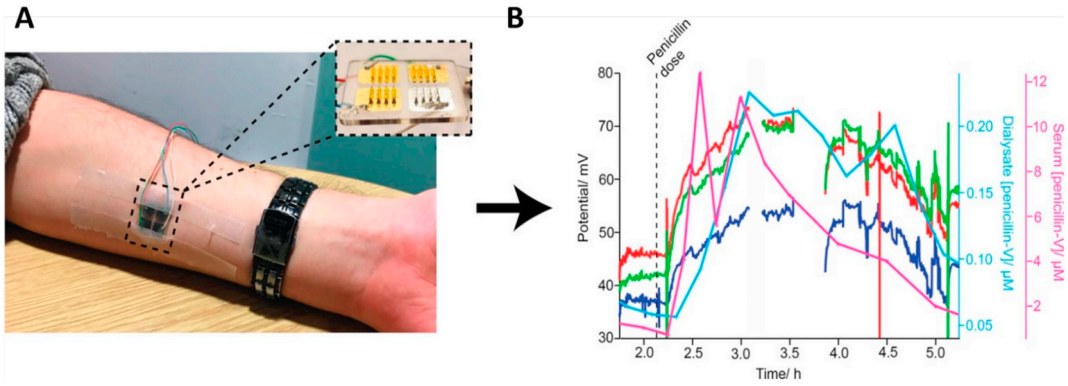

Fig. 14. A Image of individual wearing the microneedle array which consists of four metallized sets of microneedles, three coated with gold and one (bottom right-hand side in photo) with silver B in-vivo response of three β-lactamase biosensors applied to a healthy volunteer (red, green, and dark blue traces). Control response has been subtracted from each trace to remove effects of drift. Light blue: Dialysate levels of penicillin-V from a microdialysis probe inserted subcutaneously in the forearm (samples taken every 15 min), Pink: Serum levels of penicillin-V measured from blood samples taken every 15–30 min (All measurements were time aligned), [116]. (For interpretation of the references to colour in this figure legend, the reader is referred to the web version of this article.)
Reprinted by kind permission of ACS publications.

suction mechanism [30]. Needles which create a concentric opening around the needle are thought to minimize dermal compaction at the site of insertion preventing displacement of ISF from the skin [154].

Lag time is another challenge to consider. A number of studies have contributed to an understanding of the perfusion time of glucose from the blood to the ISF [170–173] with various lag times reported in the literature ranging from 5 to 25 min [173,173]. Lag time is not well studied for other target molecules mentioned through-out this review, however, advances in sensing technologies may in fact lead to answers on specific plasma-to ISF lag times. For example, Venugopal et al. developed a sensor capable of measuring alcohol levels in tissue fluid with reports of a lag time of less than 12 min between the blood and interstitial alcohol sensor readings [143].

Whilst significant advances have been made towards efficient fabrication of microneedles with common electrode materials, constructing biosensors on electrodes is not a straight-forward practice. These lab scale modification methods are not aligned with efficient device fabrication methods. In addition to this, sensor stability, sensor degradation, bio-fouling and biocompatibility are amongst some of the challenges faced by an electrochemical microneedle sensor surface. In the case of solid needles, biomolecules on the sensor surface should be entrapped/immobilized or protected by biocompatible materials to prevent leaching of biomolecules into the dermis [134]. In the case of biomarkers such as hormones, DNA and proteins, a number of steps are required in order to achieve detection as well as longer waiting times and this type of approach is not compatible with continuous monitoring applications [174–176].

At this time there is limited data on the safety and efficacy of microneedles integrated with electrochemical sensors. In a study described earlier in this review by Jina et al., skin was examined for erythema and edema following microneedle removal. No irritation was visible several days after array removal [133]. Other observations concur, and indicate that the transient erythema typically reported [89,177] after application of microneedle arrays to the skin tends to fade within a relatively short period, i.e. minutes to hours.

Almost all of the experiments presented throughout this review used a bench top potentiostat to conduct conventional electrochemical detection of analytes. In order for a microneedle sensor to find its way into

Table 4
Summary of recent electrochemical microneedle sensors fabricated via micromolding techniques.

MN[a] material - classification	MN height (μm)	Biosensor layers	Biomarker	Physiological range[b]	Reported range	Reference
Gold ink - solid	292	poly(GMA-*co*-VFc)/Urease	Urea	2.5–7.5 mM	0–2500 μM	[112]
Poly(lactic acid) and carboxyl-functionalized multiwalled carbon nanotubes nanocomposite – solid	870	N/A	Ascorbic Acid	< 0.3 mg/dL– > 0.6 mg/dL	0–1 mM	[113,166]
6% (w/v) silk was mixed with 30% (w/v) D-sorbitol and 7500 U/mL Glucose oxidase - solid	800	GOx enzyme molded into the needle during MN fabrication	Glucose	4–8 mM	1–10 mM	[114]

[a] MN (microneedle).
[b] Physiological ranges - typical values based on a healthy individual at rest.

Table 5
Summary of recent electrochemical microneedle sensors fabricated via injection molding methods.

MN material - classification	MN height (μm)	Biosensor layers	Biomarker/ drug	Physiological range [i]	Reported range	Reference
Polycarbonate – solid	1000	IrOx/beta-lactamase hydrogel/PEI	ß-Lactam	N/A	0-5 mM	[116]
Polycarbonate – solid	1000	WE1: Au/AuMWCNTs/pMB/LOx WE2: Au/AuMWCNTs/pMB/FADGDH	WE1: Lactate WE2: Glucose	Lactate: 1–2 mM Glucose: 4–8 mM	Lactate: 10–100 μM Glucose: 0–5 mM	[118],[34]
Cyclic olefin copolymer (COC), and polypyrrole (PPy) - solid	700	Au/(pTCA-GOx)/ (^{pTCA}-GOx)	Glucose	4–8 mM	0–22 mM	[117]

Table 6
Summary of recent electrochemical microneedle sensors fabricated from miscellaneous methods.

MN fabrication technology	MN height (μm)	MN material - classification	Biosensor layers	Biomarker/drug	Physiological range [i]	Reported range	Reference
Magnetorheological drawing lithography (MRDL)	600	Epoxy/novolac resin, a modified aliphatic amine curing reagent and magnetic iron particles – solid	WE 1:Ti/Au/PANI/PtNPs/UOx	WE 1: Uric Acid	Uric acid: 0.3–0.5 mM	Uric Acid: 0.1–1.2 mM	[120,136]
			WE 2:Ti/Au/PANI/PtNPs/ChOx	WE 2:Cholesterol	Cholesterol: 1–5 mM	Cholesterol: 1–12 mM	
			WE 3:Ti/Au/PANI/PtNPs/GOx	WE 3: Glucose	Glucose: 4-8 mM	Glucose: 2–12 mM	
Laser microetching	800	Stainless steel – solid	N/A	Hydrogen peroxide	Overproduction of H_2O_2 in cells occurs at $> 1 \times 10^{-3}$ M	0–10 mM	[167]
UV rapid prototyping system	1500	Eshell 200 acrylate-based polymer – hollow	Carbon paste (non-enzymatic detection WE1) mixed with tyrosinase enzyme (for enzymatic detection WE2)	Levodopa	Levels cited as 'appropriate' for therapeutic need	20-300 μM	[122,141]
CNC micromachining technique	800	Hollow (material not mentioned)	Carbon paste/Prussian Blue/HBD/NAD^+/PVC	β-hydroxybutyrate	0.6 - > 3 mM	0-1 mM and 1–10 mM	[147]
Needles glued to a stretchable PDMS substrate	1000	Stainless steel – solid	Carbon ink/CNTs/ potassium membrane cocktail	Potassium	Healthy levels: < 3.6 mM to > 5.2 mM	$10^{-3.2}$ and $10^{-1.2}$ M	[121]

a wearable patch implementation, one must develop a measurement algorithm suitable for low power consumption. With advancements in battery technology, usage of low power electronic components and low power wireless communication protocols, this appears to be a feasible milestone. However, as many of these devices are at an immature stage of development few articles have focused on the research efforts needed to integrate electrochemical sensor platforms with the necessary electronics.

5. Concluding remarks

The opportunity to attain real time molecular information from ISF remains a challenge for wearable devices. Further studies on the transdermal fluid composition as well as the molecular perfusion time from blood to the dermal ISF in human subjects is necessary for the development of future transdermal sensors. Significant advances have been made towards constructing electrochemical biosensors on microneedle platforms demonstrating their ability to gather clinically relevant information. Pharmaceuticals, metabolites and electrolytes are examples of targets which have been successfully detected with electrochemical microneedle devices in artificial ISF media as well as in human serum samples. This is the first step towards developing the sensor component for intradermal molecular monitoring. Integrated microneedle sensors have not yet reached a mature stage of development, however, a number of devices have been tested in preliminary clinical evaluation studies on human subjects. Furthermore, a select few have integrated microneedle sensors with a miniaturised potentiostat, a communication module and a power source. These devices demonstrate considerable promise for the future of wearable molecular monitoring for both personal and on-patient health care.

Funding source

The preparation of this article was supported by Science Foundation Ireland (SFI) through the Insight Centre for Data Analytics Initiative, grant numbers SFI/12/RC/2289 and SFI/12/RC/2289-P2.

Declaration of Competing Interest

The authors declare no competing financial interest.

References

[1] T. Rawson, et al., Microneedle biosensors for real-time, minimally invasive drug monitoring of phenoxymethylpenicillin: a first-in-human evaluation in healthy volunteers, Lancet Digital Health 1 (2019).
[2] D.R. Witt, et al., Windows into human health through wearables data analytics, Curr. Opin. Biomed. Eng. 9 (2019) 28–46.
[3] J. Kim, et al., Wearable biosensors for healthcare monitoring, Nat. Biotechnol. 37 (4) (2019) 389–406.
[4] T.Q. Trung, N.E. Lee, Flexible and stretchable physical sensor integrated platforms for wearable human-activity monitoringand personal healthcare, Adv. Mater. 28 (22) (2016) 4338–4372.
[5] Y. Khan, et al., Monitoring of vital signs with flexible and wearable medical devices, Adv. Mater. 28 (22) (2016) 4373–4395.
[6] R.G. Haahr, et al., An electronic patch for wearable health monitoring by reflectance pulse oximetry, IEEE Trans. Biomed. Circuits Syst. 6 (1) (2012) 45–53.
[7] S. Nagels, W. Deferme, Fabrication approaches to interconnect based devices for stretchable electronics: a review, Materials (2018) 11(3).
[8] Z. Lou, et al., Reviews of wearable healthcare systems: materials, devices and system integration, Mater. Sci. Eng. R. Rep. 140 (2020) 100523.
[9] L. Inzelberg, Y. Hanein, Electrophysiology meets printed electronics: the beginning of a beautiful friendship, Front. Neurosci. (2019) 12(992).
[10] Y. Yang, W. Gao, Wearable and Flexible Electronics for Continuous Molecular Monitoring, 48(6) (2019), pp. 1465–1491.
[11] G. Li, D. Wen, Wearable biochemical sensors for human health monitoring: sensing materials and manufacturing technologies, J. Mater. Chem. B 8 (2020) 3423–3436.
[12] C. Legner, et al., Sweat sensing in the smart wearables era: towards integrative, multifunctional and body-compliant perspiration analysis, Sensors Actuators A Phys. 296 (2019) 200–221.
[13] T. Liang, Y.J. Yuan, Wearable medical monitoring systems based on wireless

networks: a review, IEEE Sensors J. 16 (23) (2016) 8186–8199.
[14] Y. Chong, et al., Energy harvesting for wearable devices: a review, IEEE Sensors J. 19 (20) (2019) 9047–9062.
[15] D. Olczuk, R. Priefer, A history of continuous glucose monitors (CGMs) in self-monitoring of diabetes mellitus, Diabetes Metab. Syndr. Clin. Res. Rev. 12 (2) (2018) 181–187.
[16] D. Rodbard, Continuous glucose monitoring: A review of successes, challenges, and opportunities, Diabetes Technol. Ther. 18 (S2) (2016) S2 (-3-S2-13).
[17] H.S. Gill, et al., Effect of microneedle design on pain in human volunteers, Clin. J. Pain 24 (7) (2008) 585–594.
[18] G. Lee, et al., Clinical evaluation of a low-pain long microneedle for subcutaneous insulin injection, BioChip J. 12 (4) (2018) 309–316.
[19] R.A. McPherson, M.R. Pincus, J.B. Henry, Henry's Clinical Diagnosis and Management by Laboratory Methods, Philadelphia Saunders Elsevier, 2007.
[20] H. Chang, et al., A swellable microneedle patch to rapidly extract skin interstitial fluid for timely metabolic analysis, Adv. Mater. (2017) 29(37).
[21] J. Zhang, et al., In-depth proteomic analysis of tissue interstitial fluid for hepatocellular carcinoma serum biomarker discovery, Br. J. Cancer 117 (11) (2017) 1676–1684.
[22] K. Orro, et al., Development of TAP, a non-invasive test for qualitative and quantitative measurements of biomarkers from the skin surface, Biomarker Res. 2 (2014) 20.
[23] J. Hadrévi, et al., Comparative metabolomics of muscle interstitium fluid in human trapezius myalgia: an in vivo microdialysis study, Eur. J. Appl. Physiol. 113 (12) (2013) 2977–2989.
[24] T.K. Kiang, et al., Therapeutic drug monitoring in interstitial fluid: a feasibility study using a comprehensive panel of drugs, J. Pharm. Sci. 101 (12) (2012) 4642–4652.
[25] U.O. Hafeli, et al., Comparison of vancomycin concentrations in blood and interstitial fluid: a possible model for less invasive therapeutic drug monitoring, Clin. Chem. Lab. Med. 49 (12) (2011) 2123–2125.
[26] T.K.L. Kiang, S.A. Ranamukhaarachchi, M.H.H. Ensom, Revolutionizing therapeutic drug monitoring with the use of interstitial fluid and microneedles technology, Pharmaceutics 9 (4) (2017) 43.
[27] R.M. Taylor, et al., Minimally-invasive, microneedle-array extraction of interstitial fluid for comprehensive biomedical applications: transcriptomics, proteomics, metabolomics, exosome research, and biomarker identification, Lab. Anim. 52 (5) (2018) 526–530.
[28] A.L. Krogstad, et al., Microdialysis methodology for the measurement of dermal interstitial fluid in humans, Br. J. Dermatol. 134 (6) (1996) 1005–1012.
[29] W. Groenendaal, et al., Quantifying the composition of human skin for glucose sensor development, J. Diabetes Sci. Technol. 4 (5) (2010) 1032–1040.
[30] P.R. Miller, et al., Extraction and biomolecular analysis of dermal interstitial fluid collected with hollow microneedles, Commun. Biol. 1 (1) (2018) 173.
[31] S. Mitragotri, et al., Analysis of ultrasonically extracted interstitial fluid as a predictor of blood glucose levels, J. Appl. Physiol. 89 (3) (2000) 961–966.
[32] D. Adam, et al., Diffusion of cefradine and cefalothin into interstitial fluid of human volunteers with tissue cages, Infection 6 (1) (1978) S78–S81.
[33] E. Vranic, et al., Microneedle-based sensor systems for real-time continuous transdermal monitoring of analytes in body fluids, in: A. Badnjevic, R. Skrbic, L.G. Pokvic (Eds.), Proceedings of the International Conference on Medical and Biological Engineering, Cmbebih 2019, 2020, pp. 167–172.
[34] P. Bollella, et al., Minimally-invasive microneedle-based biosensor array for simultaneous lactate and glucose monitoring in artificial interstitial fluid, Electroanalysis 31 (2) (2019) 374–382.
[35] S. Sharma, et al., A pilot study in humans of microneedle sensor arrays for continuous glucose monitoring, Anal. Methods 10 (18) (2018) 2088–2095.
[36] F.E. Agrò, V. M., Physiology of body fluid compartments and body fluid movements, in: F.E. Agrò (Ed.), Body Fluid Management, Springer, Milano, 2013.
[37] J.V.M. Mathew, Physiology, Blood Plasma, StatPearls [Internet]: StatPearls Publishing, 2020.
[38] K. Aukland, G. Nicolaysen, Interstitial fluid volume: local regulatory mechanisms, Physiol. Rev. 61 (3) (1981) 556–643.
[39] R.A.A.B. Rhoades, D. R., Medical Physiology: Principles for Clinical Medicine, 3rd ed., Lippincott, Williams and Willkins, Philadelphia, 2009.
[40] E.H. Starling, On the absorption of fluids from the connective tissue spaces, J. Physiol. 19 (4) (1896) 312–326.
[41] C.C. Michel, K.P. Arkill, F.E. Curry, The revised starling principle and its relevance to perioperative fluid management, in: E. Farag, A. Kurz (Eds.), Perioperative Fluid Management, Springer International Publishing, Cham, 2016, pp. 31–74.
[42] H. Wiig, M.A. Swartz, Interstitial fluid and lymph formation and transport: physiological regulation and roles in inflammation and cancer, Physiol. Rev. 92 (3) (2012) 1005–1060.
[43] J.R. Levick, C.C. Michel, Microvascular fluid exchange and the revised Starling principle, Cardiovasc. Res. 87 (2) (2010) 198–210.
[44] K. Kretsos, G.B. Kasting, Dermal capillary clearance: physiology and modeling, Skin Pharmacol. Physiol. 18 (2) (2005) 55–74.
[45] J. Heikenfeld, et al., Accessing analytes in biofluids for peripheral biochemical monitoring, Nat. Biotechnol. 37 (4) (2019) 407–419.
[46] J.H.V. Scallan, R.J. Korthuis, Capillary Fluid Exchange: Regulation, Functions, and Pathology. Chapter 2 The Interstitium, Morgan & Claypool Life Sciences, San Rafael (CA), 2010.
[47] G. Bhave, E.G. Neilson, Body fluid dynamics: back to the future, J. Am. Soc. Nephrol. 22 (12) (2011) 2166.
[48] U.U. Shah, et al., Needle-free and microneedle drug delivery in children: a case for disease-modifying antirheumatic drugs (DMARDs), Int. J. Pharm. 416 (1) (2011) 1–11.
[49] D.J. Tobin, Biochemistry of human skin—our brain on the outside, Chem. Soc. Rev. 35 (1) (2006) 52–67.
[50] R. Wong, et al., The dynamic anatomy and patterning of skin, Exp. Dermatol. 25 (2) (2016) 92–98.
[51] L.T. Smith, K.A. Holbrook, Development of dermal connective tissue in human embryonic and fetal skin, Scan. Electron Microsc. (1982(Pt 4)) 1745–1751.
[52] M. Venus, J. Waterman, I. McNab, Basic physiology of the skin, Surgery (Oxford) 28 (10) (2010) 469–472.
[53] P.C. Benias, et al., Structure and distribution of an unrecognized interstitium in human tissues, Sci. Rep. 8 (1) (2018) 4947.
[54] National Cancer Institute, Skin Anatomy, [24-April-2020]; Available from: https://visualsonline.cancer.gov/details.cfm?imageid=4604.
[55] G. Volden, et al., Biochemical composition of suction blister fluid determined by high resolution multicomponent analysis (capillary gas chromatography—mass spectrometry and two-dimensional electrophoresis), J. Investig. Dermatol. 75 (5) (1980) 421–424.
[56] U. Kiistala, Suction blister device for separation of viable epidermis from dermis, J. Invest. Dermatol. 50 (2) (1968) 129–137.
[57] M. Müller, A. dela Peña, H. Derendorf, Issues in pharmacokinetics and pharmacodynamics of anti-infective agents: distribution in tissue, Antimicrob. Agents Chemother. 48 (5) (2004) 1441.
[58] H. Wiig, H. Noddeland, Interstitial fluid pressure in human skin measured by micropuncture and wick-in-needle, Scand. J. Clin. Lab. Invest. 43 (3) (1983) 255–260.
[59] H. Haljamäe, H. Fredén, Comparative analysis of the protein content of local subcutaneous tissue fluid and plasma, Microvasc. Res. 2 (2) (1970) 163–171.
[60] P.M. Wang, M. Cornwell, M.R. Prausnitz, Minimally invasive extraction of dermal interstitial fluid for glucose monitoring using microneedles, Diabetes Technol. Ther. 7 (1) (2005) 131–141.
[61] J.P. Bantle, W. Thomas, Glucose measurement in patients with diabetes mellitus with dermal interstitial fluid, J. Lab. Clin. Med. 130 (4) (1997) 436–441.
[62] G.D. Chisholm, et al., Concentration of antibacterial agents in interstitial tissue fluid, Brit. Med. J. 1 (5853) (1973) 569–573.
[63] J.S. Tan, et al., A method for measurement of antibiotics in human interstitial fluid, J. Infect. Dis. 126 (5) (1972) 492–497.
[64] M. Venugopal, et al., A realtime and continuous assessment of cortisol in ISF using electrochemical impedance spectroscopy, Sensors Actuators A Phys. 172 (1) (2011) 154–160.
[65] G.F. Clough, Microdialysis of large molecules, AAPS J. 7 (3) (2005) E686–E692.
[66] C.M. Huang, et al., In vivo protein sampling using capillary ultrafiltration semipermeable hollow fiber and protein identification via mass spectrometry-based proteomics, J. Chromatogr. A 1109 (2) (2006) 144–151.
[67] C. Joukhadar, M. Muller, Microdialysis: current applications in clinical pharmacokinetic studies and its potential role in the future, Clin. Pharmacokinet. 44 (9) (2005) 895–913.
[68] T.K. Kiang, U.O. Hafeli, M.H. Ensom, A comprehensive review on the pharmacokinetics of antibiotics in interstitial fluid spaces in humans: implications on dosing and clinical pharmacokinetic monitoring, Clin. Pharmacokinet. 53 (8) (2014) 695–730.
[69] R.M. Taylor, et al., Parametric study of 3D printed microneedle (MN) holders for interstitial fluid (ISF) extraction, Microsyst. Technol. 26 (2020) 2067–2073.
[70] F. Ribet, et al, Minimally Invasive and Volume-metered Extraction of Interstitial Fluid: Bloodless Point-of-Care Sampling for Bioanalyte Detection, (2020).
[71] G.-S. Liu, et al., Microneedles for transdermal diagnostics: recent advances and new horizons, Biomaterials 232 (2020) 119740.
[72] P. Dardano, I. Rea, L. De Stefano, Microneedles-based electrochemical sensors: new tools for advanced biosensing, Curr. Opin. Electrochem. 17 (2019) 121–127.
[73] A.K. Nilsson, et al., Lipid profiling of suction blister fluid: comparison of lipids in interstitial fluid and plasma, Lipids Health Dis. 18 (1) (2019) 164.
[74] J.-H. Park, M.G. Allen, M.R. Prausnitz, Biodegradable polymer microneedles: fabrication, mechanics and transdermal drug delivery, J. Control. Release 104 (1) (2005) 51–66.
[75] K. van der Maaden, et al., Microneedle-based drug and vaccine delivery via nanoporous microneedle arrays, Drug Deliv. Transl. Res. 5 (4) (2015) 397–406.
[76] M. Kim, B. Jung, J.H. Park, Hydrogel swelling as a trigger to release biodegradable polymer microneedles in skin, Biomaterials 33 (2) (2012) 668–678.
[77] M.J. Uddin, et al., Inkjet printing of transdermal microneedles for the delivery of anticancer agents, Int. J. Pharm. 494 (2) (2015) 593–602.
[78] J. Enfield, et al., In-vivo dynamic characterization of microneedle skin penetration using optical coherence tomography, J. Biomed. Opt. 15 (4) (2010) 46001.
[79] M.P. Gerstel, VA Drug Delivery Device, (1976) United States.
[80] S. Henry, et al., Microfabricated microneedles: a novel approach to transdermal drug delivery, J. Pharm. Sci. 87 (8) (1998) 922–925.
[81] C. Lee, et al., Evaluation of the anti-wrinkle effect of an ascorbic acid-loaded dissolving microneedle patch via a double-blind, placebo-controlled clinical study, Int. J. Cosmet. Sci. 38 (4) (2016) 375–381.
[82] S. Bhatnagar, K. Dave, V.V.K. Venuganti, Microneedles in the clinic, J. Control. Release 260 (2017) 164–182.
[83] E. Kim, et al., Microneedle array delivered recombinant coronavirus vaccines: immunogenicity and rapid translational development, EBioMedicine (2020) 102743.
[84] M. He, et al., Intradermal implantable PLGA microneedles for etonogestrel sustained release, J. Pharm. Sci. (2020).
[85] H. Chang, et al., Advances in the formulations of microneedles for manifold biomedical applications, Adv. Mater. Technol. 5 (4) (2020) 1900552.

[86] F. Arikat, et al., Targeting proinsulin to local immune cells using an intradermal microneedle delivery system; a potential antigen-specific immunotherapy for type 1 diabetes, J. Control. Release 322 (2020) 593–601.
[87] G.S. Guvanasen, et al., A stretchable microneedle electrode array for stimulating and measuring intramuscular electromyographic activity, IEEE Trans. Neural. Syst. Rehabil. Eng. 25 (9) (2017) 1440–1452.
[88] G. Stavrinidis, et al., SU-8 microneedles based dry electrodes for electro-encephalogram, Microelectron. Eng. 159 (2016) 114–120.
[89] C. O'Mahony, et al., Design, fabrication and skin-electrode contact analysis of polymer microneedle-based ECG electrodes, J. Micromech. Microeng. 26 (8) (2016) 084005.
[90] R. He, et al., A hydrogel microneedle patch for point-of-care testing based on skin interstitial fluid, Adv. Healthcare Mater. 9 (4) (2020) 1901201.
[91] Y. Wang, et al., Towards a transdermal membrane biosensor for the detection of lactate in body fluids, Sensors Actuators B Chem. 308 (2020) 127645.
[92] FDA, 510k Summary K092746, Available from: https://www.accessdata.fda.gov/scripts/cdrh/cfdocs/cfpmn/pmn.cfm?ID=K092746.
[93] NanoPass Technologies Ltd, MicronJet600 Advanced Intradermal Solution, [02-04-2020]; Available from: https://www.nanopass.com/product/.
[94] M.R. Prausnitz, Engineering microneedle patches for vaccination and drug delivery to skin, Ann. Rev. Chem. Biomol. Eng. 8 (1) (2017) 177–200.
[95] clinicaltrials.gov, Efficacy & Safety of Abaloparatide-Solid Microstructured Transdermal System in Postmenopausal Women With Osteoporosis, (2019) Online.
[96] T.M. Blicharz, et al., Microneedle-based device for the one-step painless collection of capillary blood samples, Nat. Biomed. Eng. 2 (3) (2018) 151–157.
[97] Dermaroller®GmbH, About Us, [18-04-2020]; Available from: https://www.original-dermaroller.de/en/medical-care/about-us/.
[98] 3 M Science Applied to Life, About 3M Microneedle Drug Delivery Systems, [02-04-2020]; Available from: https://www.3m.com/3M/en_US/drug-delivery-systems-us/technologies/microneedle/.
[99] Zimmer and Peacock, Microneedle Arrays, [02-04-2020]; Available from: https://www.zimmerpeacocktech.com/products/electrochemical-sensors/microneedle-arrays/.
[100] Zosano Pharma, Intracutaneous Microneedle System, [03-04-2020]; Available from: https://www.zosanopharma.com/technology/.
[101] R.F. Donnelly, T.R. Raj Singh, A.D. Woolfson, Microneedle-based drug delivery systems: microfabrication, drug delivery, and safety, Drug Deliv. 17 (4) (2010) 187–207.
[102] L. Xie, et al., Engineering microneedles for therapy and diagnosis: a survey, Micromachines (2020) 11(3).
[103] R. Ali, et al., Transdermal microneedles—a materials perspective, AAPS PharmSciTech 21 (1) (2019) 12.
[104] T. Waghule, et al., Microneedles: a smart approach and increasing potential for transdermal drug delivery system, Biomed. Pharmacother. 109 (2019) 1249–1258.
[105] S. Duarah, M. Sharma, J. Wen, Recent advances in microneedle-based drug delivery: special emphasis on its use in paediatric population, Eur. J. Pharm. Biopharm. 136 (2019) 48–69.
[106] E. Larrañeta, et al., Microneedle arrays as transdermal and intradermal drug delivery systems: materials science, manufacture and commercial development, Mater. Sci. Eng. 104 (2016) 1–32.
[107] W. Yu, et al., Fabrication of biodegradable composite microneedles based on calcium sulfate and gelatin for transdermal delivery of insulin, Mater. Sci. Eng. C 71 (2017) 725–734.
[108] Y. Yoon, et al., Fabrication of a microneedle/CNT hierarchical micro/nano surface electrochemical sensor and its in-vitro glucose sensing characterization, Sensors 13 (12) (2013).
[109] Y. Li, et al., Fabrication of sharp silicon hollow microneedles by deep-reactive ion etching towards minimally invasive diagnostics, Microsyst. Nanoeng. 5 (1) (2019) 41.
[110] C. O'Mahony, et al., Microneedle-based electrodes with integrated through-silicon via for biopotential recording, Sensors Actuators A Phys. 186 (2012) 130–136.
[111] K. Dawson, et al., Fully integrated on-chip nano-electrochemical devices for electroanalytical applications, Electrochim. Acta 115 (2014) 239–246.
[112] M. Senel, M. Dervisevic, N.H. Voelcker, Gold microneedles fabricated by casting of gold ink used for urea sensing, Mater. Lett. 243 (2019) 50–53.
[113] E. Skaria, et al., Poly(lactic acid)/carbon nanotube composite microneedle arrays for dermal biosensing, Anal. Chem. 91 (7) (2019) 4436–4443.
[114] L. Zhao, et al., Silk/polyols/GOD microneedle based electrochemical biosensor for continuous glucose monitoring, RSC Adv. 10 (11) (2020) 6163–6171.
[115] K. Takeuchi, et al., Microfluidic chip to interface porous microneedles for ISF collection, Biomed. Microdevices 21 (1) (2019) 28.
[116] S.A.N. Gowers, et al., Development of a minimally invasive microneedle-based sensor for continuous monitoring of β-lactam antibiotic concentrations in vivo, ACS Sensors 4 (4) (2019) 1072–1080.
[117] K.B. Kim, et al., Continuous glucose monitoring using a microneedle array sensor coupled with a wireless signal transmitter, Sensors Actuators B Chem. 281 (2019) 14–21.
[118] A.E.G. Cass, S. Sharma, Chapter fifteen - microneedle enzyme sensor arrays for continuous in vivo monitoring, in: R.B. Thompson, C.A. Fierke (Eds.), Methods in Enzymology, Academic Press, 2017, pp. 413–427.
[119] Z. Chen, et al., Rapidly fabricated microneedle arrays using magnetorheological drawing lithography for transdermal drug delivery, ACS Biomater. Sci. Eng. 5 (10) (2019) 5506–5513.
[120] Z. Chen, et al., Rapid fabrication of microneedles using magnetorheological drawing lithography, Acta Biomater. 65 (2018) 283–291.
[121] M. Parrilla, et al., Wearable all-solid-state potentiometric microneedle patch for intradermal potassium detection, Anal. Chem. 91 (2) (2019) 1578–1586.
[122] J.R. Windmiller, et al., Microneedle array-based carbon paste amperometric sensors and biosensors, Analyst 136 (9) (2011) 1846–1851.
[123] A.R. Johnson, et al., Single-step fabrication of computationally designed microneedles by continuous liquid Interface production, PLoS One 11 (9) (2016) e0162518.
[124] T.M. Rawson, et al., Towards a minimally invasive device for beta-lactam monitoring in humans, Electrochem. Commun. 82 (2017) 1–5.
[125] S. Sharma, et al., Rapid, low cost prototyping of transdermal devices for personal healthcare monitoring, Sens. Bio-Sens. Res. 13 (2016) 104–108.
[126] C. Barrett, et al., Novel surface modified polymer microneedle based biosensors for interstitial fluid glucose detection, IEEE Sens. (2019) 1–4.
[127] S. Wang, et al., Insulin-loaded silk fibroin microneedles as sustained release system, ACS Biomater. Sci. Eng. 5 (4) (2019) 1887–1894.
[128] K.J. Krieger, et al., Simple and customizable method for fabrication of high-aspect ratio microneedle molds using low-cost 3D printing, Microsyst. Nanoeng. 5 (1) (2019) 42.
[129] S.A. Ranamukhaarachchi, et al., Integrated hollow microneedle-optofluidic biosensor for therapeutic drug monitoring in sub-nanoliter volumes, Sci. Rep. 6 (1) (2016) 29075.
[130] E.V. Mukerjee, et al., Microneedle array for transdermal biological fluid extraction and in situ analysis, Sensors Actuators A Phys. 114 (2–3) (2004) 267–275.
[131] B.Q. Tran, et al., Proteomic Characterization of Dermal Interstitial Fluid Extracted Using a Novel Microneedle-Assisted Technique. 17(1) (2018), pp. 479–485.
[132] E. Caffarel-Salvador, et al., Hydrogel-forming microneedle arrays allow detection of drugs and glucose in vivo: potential for use in diagnosis and therapeutic drug monitoring, PLoS One 10 (12) (2015) e0145644.
[133] A. Jina, et al., Design, development, and evaluation of a novel microneedle array-based continuous glucose monitor, J. Diabetes Sci. Technol. 8 (3) (2014) 483–487.
[134] A.M.V. Mohan, et al., Continuous minimally-invasive alcohol monitoring using microneedle sensor arrays, Biosens. Bioelectron. 91 (2017) 574–579.
[135] F. Ribet, G. Stemme, N. Roxhed, Real-time intradermal continuous glucose monitoring using a minimally invasive microneedle-based system, Biomed. Microdevices 20 (4) (2018) 101.
[136] J. Gao, et al., Simultaneous detection of glucose, uric acid and cholesterol using flexible microneedle electrode array-based biosensor and multi-channel portable electrochemical analyzer, Sensors Actuators B Chem. 287 (2019) 102–110.
[137] C. Barrett, et al., Development of low cost rapid fabrication of sharp polymer microneedles for in vivo glucose biosensing applications, ECS J. Solid State Sci. Technol. 4 (10) (2015) S3053–S3058.
[138] P.P. Samant, M.R. Prausnitz, Mechanisms of sampling interstitial fluid from skin using a microneedle patch, Proc. Natl. Acad. Sci. 115 (18) (2018) 4583–4588.
[139] A.V. Romanyuk, et al., Collection of analytes from microneedle patches, Anal. Chem. 86 (21) (2014) 10520–10523.
[140] E.P.-C.A.C. Ford, Flash glucose monitoring system for diabetes, CADTH Issues in Emerging Health Technologies, C.A.f.D.a.T.i. Health, Ottawa, 2017.
[141] K.Y. Goud, et al., Wearable electrochemical microneedle sensor for continuous monitoring of levodopa: toward Parkinson management, ACS Sensors 4 (8) (2019) 2196–2204.
[142] H.-R. Jeong, et al., Considerations in the use of microneedles: pain, convenience, anxiety and safety, J. Drug Target. 25 (1) (2017) 29–40.
[143] M. Venugopal, et al., Clinical evaluation of a novel interstitial fluid sensor system for remote continuous alcohol monitoring, IEEE Sensors J. 8 (1) (2008) 71–80.
[144] A.H. Bretag, Synthetic interstitial fluid for isolated mammalian tissue, Life Sci. 8 (5) (1969) 319–329.
[145] B. Ciui, et al., Wearable wireless tyrosinase bandage and microneedle sensors: toward melanoma screening, Adv. Healthcare Mater. 7 (7) (2018) 1701264.
[146] M.P. R., et al., Microneedle-Based Transdermal Sensor for On-Chip Potentiometric Determination of K+. Advanced Healthcare Materials, 3(6) (2014), pp. 876–881.
[147] H. Teymourian, et al., Microneedle-based detection of ketone bodies along with glucose and lactate: toward real-time continuous ISF monitoring of diabetic ketosis/ketoacidosis, Anal. Chem. 92 (2) (2019) 2291–2300.
[148] A. Abellán-Llobregat, et al., A stretchable and screen-printed electrochemical sensor for glucose determination in human perspiration, Biosens. Bioelectron. 91 (2017) 885–891.
[149] T. Glennon, et al., 'SWEATCH': A wearable platform for harvesting and analysing sweat sodium content, Electroanalysis 28 (6) (2016) 1283–1289.
[150] J. Kim, et al., Non-invasive mouthguard biosensor for continuous salivary monitoring of metabolites, Analyst 139 (7) (2014) 1632–1636.
[151] J.R. Sempionatto, et al., Eyeglasses based wireless electrolyte and metabolite sensor platform, Lab Chip 17 (10) (2017) 1834–1842.
[152] J. Kim, et al., Wearable smart sensor systems integrated on soft contact lenses for wireless ocular diagnostics, Nat. Commun. 8 (2017) 14997.
[153] P. Khanna, et al., Microneedle-based automated therapy for diabetes mellitus, J. Diabetes Sci. Technol. 2 (6) (2008) 1122–1129.
[154] S.R. Chinnadayyala, K.D. Park, S. Cho, Editors' choice—review—in vivo and in vitro microneedle based enzymatic and non-enzymatic continuous glucose monitoring biosensors, ECS J. Solid State Sci. Technol. 7 (7) (2018) Q3159–Q3171.
[155] A. El-Laboudi, et al., Use of microneedle array devices for continuous glucose monitoring: a review, Diabetes Technol. Ther. 15 (1) (2012) 101–115.
[156] S. Sharma, et al., Evaluation of a minimally invasive glucose biosensor for continuous tissue monitoring, Anal. Bioanal. Chem. 408 (29) (2016) 8427–8435.
[157] P. Adolfsson, et al., Selecting the appropriate continuous glucose monitoring system - a practical approach, Eur. Endocrinol. 14 (1) (2018) 24–29.
[158] S.R. Chinnadayyala, I. Park, S. Cho, Nonenzymatic determination of glucose at

near neutral pH values based on the use of nafion and platinum black coated microneedle electrode array, Mikrochim. Acta 185 (5) (2018) 250.
[159] O.V. Soldatkina, et al., A novel amperometric glutamate biosensor based on glutamate oxidase adsorbed on Silicalite, Nanoscale Res. Lett. 12 (1) (2017) 260.
[160] J.R. Windmiller, et al., Bicomponent microneedle array biosensor for minimally-invasive glutamate monitoring, Electroanalysis 23 (10) (2011) 2302–2309.
[161] A. Caliò, Polymeric microneedles based enzymatic electrodes for electrochemical biosensing of glucose and lactic acid, Sensors Actuators B Chem. 236 (2016) 343–349.
[162] N. Nikolaus, B. Strehlitz, Amperometric lactate biosensors and their application in (sports) medicine, for life quality and wellbeing, Microchim. Acta 160 (1) (2008) 15–55.
[163] K. Rathee, et al., Biosensors based on electrochemical lactate detection: a comprehensive review, Biochem. Biophys. Rep. 5 (2016) 35–54.
[164] L.W. Andersen, et al., Etiology and therapeutic approach to elevated lactate levels, Mayo Clin. Proc. 88 (10) (2013) 1127–1140.
[165] P. Bollella, et al., Microneedle-based biosensor for minimally-invasive lactate detection, Biosens. Bioelectron. 123 (2019) 152–159.
[166] A.F. Hagel, et al., Plasma concentrations of ascorbic acid in a cross section of the German population, J. Int. Med. Res. 46 (1) (2018) 168–174.
[167] Q. Jin, et al., Reduced graphene oxide nanohybrid–assembled microneedles as mini-invasive electrodes for real-time transdermal biosensing, Small 15 (6) (2019) 1804298.
[168] E. Cengiz, W.V. Tamborlane, A tale of two compartments: interstitial versus blood glucose monitoring, Diabetes Technol. Ther. 11 (Suppl. 1) (2009) S11–S16.
[169] C. Scuffi, Interstitium versus blood equilibrium in glucose concentration and its impact on subcutaneous continuous glucose monitoring systems, Eur. Endocrinol. 10 (1) (2014) 36–42.
[170] K. Rebrin, N.F. Sheppard Jr., G.M. Steil, Use of subcutaneous interstitial fluid glucose to estimate blood glucose: revisiting delay and sensor offset, J. Diabetes Sci. Technol. 4 (5) (2010) 1087–1098.
[171] T. Koutny, Blood glucose level reconstruction as a function of transcapillary glucose transport, Comput. Biol. Med. 53 (2014) 171–178.
[172] D. Barry Keenan, et al., Interstitial fluid glucose time-lag correction for real-time continuous glucose monitoring, Biomed. Signal Process. Contr. 8 (1) (2013) 81–89.
[173] T. Siegmund, et al., Discrepancies between blood glucose and interstitial glucose-technological artifacts or physiology: implications for selection of the appropriate therapeutic target, J. Diabetes Sci. Technol. 11 (4) (2017) 766–772.
[174] R. Esfandyarpour, et al., Microneedle biosensor: a method for direct label-free real time protein detection, Sensors Actuators B Chem. 177 (2013) 848–855.
[175] D. Kinnamon, et al., Portable biosensor for monitoring cortisol in low-volume perspired human sweat, Sci. Rep. 7 (1) (2017) 13312.
[176] S. Teixeira, et al., Chitosan/AuNPs modified graphene electrochemical sensor for label-free human chorionic gonadotropin detection, Electroanalysis 26 (12) (2014) 2591–2598.
[177] M. Kim, et al., Curved microneedle array-based sEMG electrode for robust long-term measurements and high selectivity, Sensors (2015) 15(7).